Proteomic, Cellular, and Network Analyses Reveal New DUSP3 Interactions with Nucleolar Proteins in HeLa Cells

ARTICLE *in* JOURNAL OF PROTEOME RESEARCH · NOVEMBER 2013

Impact Factor: 4.25 · DOI: 10.1021/pr400867j · Source: PubMed

Journal of proteome research

Article

pubs.acs.org/jpr

Proteomic, Cellular, and Network Analyses Reveal New DUSP3 Interactions with Nucleolar Proteins in HeLa Cells

Karine Panico[†] and Fabio Luis Forti*[,‡,§]

[†]Centro de Ciências Naturais e Humanas, Universidade Federal do ABC, Rua Santa Adélia, 166, Bairro Bangu, Santo Andre-SP 09210-170, Brazil

[‡]Laboratório de Sinalização em Sistemas Biomoleculares, Departamento de Bioquímica, Instituto de Química, Universidade de São Paulo, Av. Prof. Lineu Prestes, 748 -B.09i, Sl.922, Sao Paulo-SP 05508-000, Brazil

Supporting Information

ABSTRACT: DUSP3 (or *Vaccinia virus* phosphatase VH1-related; VHR) is a small dual-specificity phosphatase known to dephosphorylate c-Jun N-terminal kinases and extracellular signal-regulated kinases. In human cervical cancer cells, DUSP3 is overexpressed, localizes preferentially to the nucleus, and plays a key role in cellular proliferation and senescence triggering. Other DUSP3 functions are still unknown, as illustrated by recent and unpublished results from our group showing that this enzyme mediates DNA damage response or repair processes. In this study, we sought to identify new interactions between DUSP3 and proteins directly or indirectly involved in or correlated with its biological roles in HeLa cells exposed to gamma or UV radiation. By using GST-DUSP as bait, we pulled down interacting proteins and identified them by LC−MS/MS. Of the 46 proteins obtained, six hits were extensively validated by immune techniques; the proteins Nucleophosmin, HnRNP C1/C2, and Nucleolin were the most promising targets found to directly interact with DUSP3. We then analyzed the DUSP3 interactomes using physical protein−protein interaction networks using our hits as the seed list. The validated hits as well as unvalidated hits fluctuated on the DUSP3 interactomes of HeLa cells, independent of the time post radiation, which confirmed our proteomic and experimental data and clearly showed the proximity of DUSP3 to proteins involved in processes intimately related to DNA repair and senescence, such as Ku70 and Tert, via interactions with nucleolar proteins, which were identified in this study, that regulate DNA/RNA structure and functions.

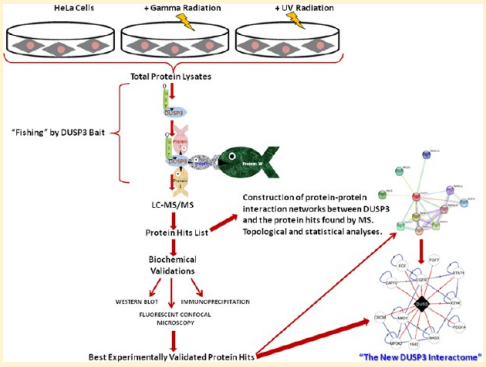

KEYWORDS: *Dual-specificity phosphatase 3 (DUSP3/VHR), protein tyrosine phosphatase (PTP), physical protein−protein interaction (PPPI), proteomics, mass spectrometry, interactomes, nucleophosmin (NPM), HnRNP C1/C2, nucleolin (NUCL), DNA damage and repair*

INTRODUCTION

The phosphorylation of proteins on tyrosine residues is an important post-translational modification that cells use to regulate signal transduction. Protein tyrosine kinases (PTKs) and protein tyrosine phosphatases (PTPs) are essential for several cellular processes, including cell growth, differentiation, metabolism, the cell cycle, cell−cell communication, cell migration, gene transcription, immune responses, and cell survival.[1,2]

Among the four PTP classes, which include classical and nonclassical PTPs (dual-specificity phosphatases), there is a subclass, termed atypical DUSPs, that harbors the consensus PTP catalytic domain consensus and can dephosphorylate tyrosine and threonine residues; atypical DUSPs lack the N-terminal CH2 domain that is often found in mitogen-activated protein kinase (MAPK) phosphatases (MKPs). Certain atypical DUSPs were originally grouped as MKPs because it was thought that they played a similar role in the regulation of MAPK cascades.[3] In addition, the dual-specificity phosphatases may use other substrates not containing pTyr and pSer or pThr,[2] such as carbohydrates[4] and lipids.[5] Although it is known that certain atypical DUSPs regulate MAPKs, it is becoming increasingly clear that atypical DUSPs may have different substrate specificities and physiological roles from those of typical MKPs.[3]

This subclass of atypical DUSPs includes vaccinia virus phosphatase VH1-related (VHR), or DUSP3, which exhibits preferential nuclear localization and regulates cell-cycle progression in many cell types. DUSP3 has been shown to be overexpressed under stress conditions and in cervical,[6,7] prostate,[8] and breast[9] cancer cells. This protein dephosphorylates and thus inactivates extracellular signals that regulate c-Jun N-terminal kinases (JNK1/2) and extracellular signal-regulated kinases (ERK1/2) through specific and strong binding to a phosphotyrosine residue within the activation loop of these MAPKs − more specifically, inside the pT-X-pY motif.[3] The 3-D structure of DUSP3was determined by X-ray

Received: August 23, 2013
Published: November 18, 2013

crystallography, showing a single DUSP catalytic domain (DSPc) containing a "loop" between residues 123 and 131, with the active site consensus sequence His-Cys-X-X-Gly-X-X-Arg(Ser/Thr) and the catalytic residue at position Cys^{124} as the main site for catalysis.[10]

MAPKs mediate major signaling pathways triggered by extracellular growth factors, cytokines, or stresses and regulate cellular processes such as differentiation, proliferation, and apoptosis.[11] However, the exposure of cellular organisms to stress conditions, such as ionizing radiation (IR) (e.g., gamma or X-rays) and nonionizing (e.g., ultraviolet A, B, or C) radiation, can lead to various types of DNA damage, including single- (SSB) or double-strand breaks (DSB), which are sensed by a cascade of events termed the DNA damage response (DDR) that controls the cellular responses to damage.[12] It is known that the P38,[13] ERK,[14] and JNK[14,15] MAPKs can positively or negatively modulate DDR. However, the mechanisms are not completely understood.

In addition to its regulation of proliferation and apoptosis in human tumorigenic cells through MAPK downregulation, the loss of DUSP3 has been shown to induce G1-S and G2-M arrest and consequent cellular senescence in cervical cancer cells, including the downregulation of telomerase activity.[6] Cellular evidence of the participation of DUSP3 in DNA damage/repair processes has also been shown by colocalization in phospho-H2AX foci;[16] however, the molecular mechanisms remain to be fully investigated.

Hence, the present study aims to identify new interactions between DUSP3 and other proteins (except for MAPK) that might be involved, either directly or indirectly, in DDR processes, such as DNA repair, cell cycle arrest, apoptosis, senescence, and other processes, in HeLa cells exposed to stress conditions caused by gamma and ultraviolet radiation. Our investigation focuses on the initial identification of new protein targets or partners of DUSP3 through proteomics using GST-tagged DUSP3as the bait in pull-down experiments performed using cell lysates, followed by biochemical validations using different techniques. These new interactions were then confirmed using systems biology approaches to investigate topological and centrality aspects of the interactomes containing DUSP3 before and after this study.

EXPERIMENTAL PROCEDURES

Cell Culture

HeLa cells (CCL-2, American Type Culture Collection) were cultured in DME medium (Invitrogen, Carlsbad, CA) with streptomycin and ampicillin (Invitrogen) containing 10% fetal bovine serum (FBS; Cultilab, Campinas, SP, Brazil) in a 37 °C incubator MCO-19AICUV-PA (Sanyo, Tokyo, Japan) with a humidified 5% CO_2 atmosphere. The cells were maintained in culture at early passages (up to 10), subcultured every 3 days and plated in dishes of varying diameter according to the experimental protocols. The cells were regularly submitted to two different treatments: first, using 5 Gy γ radiation from a Cobalt-60 source [Co^{60}-GammaCel 220, Atomic Energy of Canada Limited (AECL), Ontario, Canada] at the Institute of Energy and Nuclear Research (IPEN, São Paulo-SP, Brazil); and second, using ultraviolet radiation in the UVA (597 J/m^2 at 365 nm), UVB (90 J/m2 at 302 nm), and UVC (6 J/m2 at 254 nm) ranges with specific lamps continuously calibrated for wavelength and intensity using a dosimeter (VLX-3W, Vilber Lourmat).

Cell Lysates for Pull-Down, Western Blot and Co-Immunoprecipitation Experiments

The HeLa cell suspension was seeded in 100 mm diameter dishes at 50−75% confluence 24 h after being submitted to the aforementioned UV or γ radiation treatments. Cell lysates were obtained using RIPA buffer (50 mM Tris pH 7.2, 1% Triton X-100, 0.5% sodium deoxycholate, 0.1% SDS, 500 mM NaCl, and 10 mM $MgCl_2$, Sigma) containing a protease inhibitor cocktail (2 μg/mL aprotinin, 2 μg/mL leupeptin, 1 mM DTT, 1 mM PMSF, 2 μg/mL pepstatin, Sigma).

Pull-Down Assay

E. coli cultures (strain BL-21), previously transformed with empty pGEX-4T1 vector (GE Healthcare) or pGEX-4T1 containing either wild-type DUSP3 cDNA or an active-site mutant (DUSP3-C124S), were grown in LB (15% Bacto Tryptone, 5% yeast extract, and 15% NaCl, Sigma) culture medium. The cells were induced with 0.5 mM IPTG for 2 h at 37 °C to obtain bacterial cell lysates overexpressing the GST-DUSP3-WT or GST-DUSP3-C124S fusion proteins or the GST protein alone as a control. Bacterial cell suspensions were sonicated on ice using eight 2 min pulses. The supernatants containing the soluble bacterial proteins were incubated with glutathione-sepharose beads (4B, GE Healthcare) to pull down the GST-fused proteins, which were then resolved using SDS-PAGE and quantified using the Bradford (Bio-Rad, Hercules, CA) method. Beads were first washed with ice-cold PBS, followed by centrifugation for 3 min at 3000 rpm at 4 °C and subsequently incubated with 250 μL of bacterial lysate containing the GST-DUSP3 fusion protein for 1 h with stirring. After another wash of the beads with RIPA buffer under the same conditions as above, the beads were incubated with HeLa cell lysates (0.5 mg of total protein) for 1 h and washed again with RIPA buffer under the same conditions as previously described (adapted from ref 17). The purified complexes were separated using 10% SDS-PAGE and visualized with silver staining (0.2%). In brief, the gels were fixed for 2 h in a 1:1 (v/v) solution of ethanol/acetic acid and for more than 1.5 h in a solution containing ethanol, glutaraldehyde (25%), sodium acetate, and sodium thiosulphate (Synth, Sao Paulo, Brazil). Subsequently, the gels were incubated in silver nitrate (0.002 g/mL) and formaldehyde (35%) (Synth) for 20 min and developed in a solution containing sodium carbonate (0.068 g/mL) and formaldehyde (35%). Finally, the reaction was stopped with 0.05 M EDTA (adapted from ref 18).

Protein Digestion and Mass Spectrometry Analysis

The SDS-PAGE gels were scanned on a GE Healthcare Image Scanner III (resolution 300 dpi, red filter and transparent mode) and scanned for differential bands in the treated samples (gamma and ultraviolet A, B, and C radiation) compared with control or untreated samples. All conditions were compared with the empty vector (pGEX-4T1), with or without incubation with untreated cell lysate and to the fusion protein (GST-DUSP3) bound to the glutathione-sepharose beads. The selected bands were then excised from the gel and destained for 2 h at room temperature in 0.5 mL of 50% methanol and 5% acetic acid to remove SDS (10%) and then left for 1 h in the same solution before the dehydration step with 200 μL of acetonitrile (100%) for 5 min and complete drying in a vacuum centrifuge. The proteins were reduced by the addition of 30 μL of a 10 mM DTT solution (1.5 mg DTT in 1 mL of 100 mM ammonium bicarbonate) and alkylated using 30 μL of 50 mM iodoacetamide solution (10 mg of iodoacetamide in 1 mL of

dx.doi.org/10.1021/pr400867j | J. Proteome Res. 2013, 12, 5851−5866

100 mM ammonium bicarbonate), both for 30 min at room temperature. To exchange the buffer, we hydrated the gel pieces in 100 μL of 100 mM ammonium bicarbonate for 10 min and dehydrated them in 200 μL of acetonitrile (100%) for 5 min. The gel pieces were again rehydrated with 200 μL of 100 mM ammonium bicarbonate for 10 min and then dehydrated in 200 μL of acetonitrile (100%) for 5 min. Finally, the dehydrated gel pieces were completely dried in a vacuum centrifuge and rehydrated in 20 ng/μL of sequencing-grade modified trypsin (Promega, Madison, WI) and 50 mM ammonium bicarbonate for 30 min on ice. Any excess trypsin solution was removed, and the digestion was carried out overnight at 37 °C. The peptides produced in the digestion were collected by successive extractions with 30 μL of 5% formic acid (first extraction solution), then with 5% formic acid and acetonitrile (50%) (second extraction solution); extracts were combined in a 0.6 mL microcentrifuge tube. The total extract was concentrated in a vacuum centrifuge until ∼1 μL remained. The resulting peptides were separated by a C18 (100 μm × 100 mm) RP-nanoUPLC (nanoAcquity, Waters) apparatus coupled to a Q-T of Ultima mass spectrometer (Waters) with a nanoelectrospray source at a flow rate of 0.6 μL/min. The gradient was 2−90% acetonitrile in 0.1% formic acid over 45 min for the digested proteins and 60 min for endogenous peptides. The nanoelectrospray voltage was set to 3.5 kV, with a cone voltage and source temperature of 30 V and 100 °C, respectively. The instrument was operated in the "top three" mode, in which one MS spectrum is acquired, followed by MS/MS of the three most intense peaks.[19] These analyses were performed at the National Laboratory of Biosciences (LNBio) at the National Center for Research in Energy and Materials (CNPEM) in Campinas-SP, Brazil. For the identification of the proteins analyzed, data processing was performed using MASCOT software. The setup of the ideal parameters in our analysis was as follows: SwissProt (database), trypsin (enzyme), *Homo sapiens* (taxonomy), carbamidomethyl (variable modifications), peptide tolerance − 1.2 Da, MS/MS tolerance − 0.6 Da, peptide charge (+2, +3, and +4), and Mascot generic (data format). The instrument used in the analyses was ESI-QUAD-TOF. According to MASCOT probability analysis, only significant hits ($p < 0.05$) were accepted.

Immunoblotting

The proteins identified by MS after isolation by the "pull down" technique previously described were validated by Western blotting. The cell lysates were resolved on 10 or 12% SDS-PAGE gels, transferred onto Hybond-C nitrocellulose membranes (GE Healthcare) using the semidry transfer buffer (25 mM Tris pH 7.5, 0.2 M glycine, and 20% methanol) in a trans-blot TE77 PWR model (Amersham Biosciences), and then blocked for 1 h at room temperature in Tris-buffered saline with Tween 20 (TBST) and 5% nonfat milk. The following specific antibodies were used for the immunoblots: (A) mouse anti-NUCL (clone 3G4B2; Upstate; Millipore-Merck), anti-PHB (Ab-1 Clone II-14−10; Labvision, Thermo Scientific) and anti-NPM (monoclonal anti-B23 clone FC82291; Sigma); (B) rabbit anti-HnRNP C1/C2 (sc-15386 H-105; Santa Cruz Biotechnology, Santa Cruz, CA) and anti-vimentin (anti-VIME) (sc-7557 C-20; Santa Cruz Biotechnology); and (C) goat antihistone H1 (sc-34464N-16; Santa Cruz Biotechnology). Incubations were all performed in Tris-buffered saline with (0.01 g/mL) Tween 20 (0.1%; TBST) using antibody dilutions of 1:1000 and incubation times varying between 2 h at room temperature to overnight (18 h) at 4 °C. After three 5 min washes in TBST, the nitrocellulose membranes were incubated for 1 h at room temperature with antimouse, antirabbit, or antigoat antibodies conjugated with IRDye (Li-Cor, Lincoln, NE) or Alexa-Fluor (Invitrogen) for wavelengths of 680 or 800 nm at dilutions of 1:15 000. The membranes were scanned with an Odyssey Infrared Imaging System (LI-COR Biosciences, Lincoln, NE) and quantified using Odyssey software (version 3.0).

Immunofluorescence

HeLa cells grown on glass coverslips after treatment with 5 Gy γ radiation were fixed with the fixing solution (3% formaldehyde, 37% solution, 3% paraformaldehyde, 2% sucrose in PBS) (Synth) for 10 min and then permeabilized (0.5% Triton X-100, 6.84% sucrose, 3 mM $MgCl_2$ in PBS) (Synth) for 5 min on ice. Next, the cells were incubated with 1:500 dilutions of the following primary antibodies for 2 h at room temperature: mouse anti-DUSP3 (BD Biosciences), goat anti-DUSP3 (Santa Cruz Biotechnology), mouse anti-NUCL (Millipore-Merck), mouse anti-NPM (Sigma), mouse anti-PHB, rabbit anti-HnRNP C1/C2 (Santa Cruz Biotechnology), rabbit anti-VIME (Santa Cruz Biotechnology), and goat antihistone H1 (Santa Cruz Biotechnology). The following secondary antibodies were diluted 1:500 in PBS and incubated for 1 h at room temperature: donkey antigoat (Alexa Fluor 488 nm) for DUSP3 (antigoat); donkey antimouse (Alexa Fluor, 568 nm) for NUCL, NPM, and PHB; goat antimouse (Alexa Fluor 488 nm) for DUSP3 and goat antirabbit (Alexa Fluor, 568 nm) for HnRNP C1/C2 and VIME; and donkey antimouse (Alexa Fluor, 488 nm) and goat antirabbit (Alexa Fluor, 568 nm) for DUSP3 (antimouse) and histone H1, respectively. The coverslips were mounted using the Vectashield (Vector Laboratories, Burlingame, CA) fixing agent containing DAPI, and the cells were observed under a confocal microscope (Zeiss LSM 510-Meta, Germany). The image acquisition and analyses were performed using Start LSM Image Browser software (Zeiss, Germany).

Immunoprecipitation

Lysates of HeLa cells (0.5 mg) with or without a 5 Gy γ radiation treatment (obtained as previously described) were incubated with the primary antibody anti-DUSP3 (Santa Cruz Biotechnology) in RIPA buffer for 16 h at 4 °C under rotation and subsequently (the next day) incubated for an additional 1.5 h with the Protein A/G PLUS-agarose immunoprecipitation reagent (Santa Cruz Biotechnology). The complexes were then centrifuged, washed five times in RIPA buffer with alternate centrifugations (3000 rpm, 3 min), and separated on 12% SDS-PAGE gels. The gels were transferred onto membranes with the same buffer and semidry trans-blot as previous, and Western blotting was performed to confirm the DUSP3 interactions with NUCL, NPM, HnRNP, Histone H1, PHB and VIME proteins, as previously described.

Design of Physical Protein−Protein Interaction Networks and Topological Analyses

The data obtained from proteomic analyses of the human HeLa cell line with or without ionizing (γ radiation) or nonionizing (UV) radiation treatments were used to design potential networks with other proteins in the context of physical protein−protein interactions (PPPIs). For this purpose, we started the data mining and network design using DUSP3

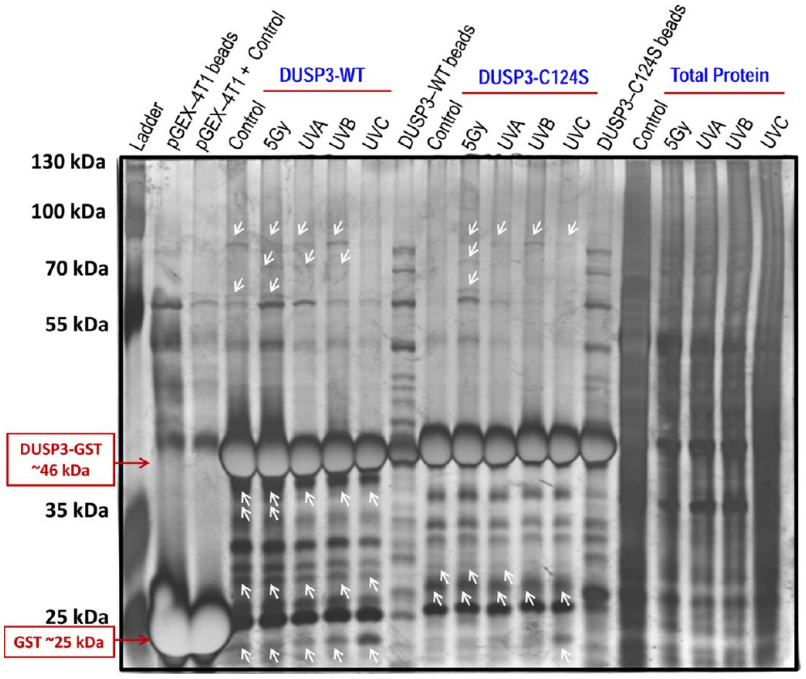

Figure 1. HeLa cell lysates obtained 30 min after the indicated treatments with gamma or UV radiation were pulled down using DUSP-GST and resolved on 10% SDS-PAGE gels, followed by silver staining to visualize, isolate, and identify protein bands. The gel shown is representative of three independent pull-down experiments, and the white arrows indicate examples of differential protein bands not found in the controls (GST pull-down or DUSP3-GST-isolated beads) suitable to be excised and submitted to MS analyses.

(bait) plus 45 high-scoring human proteins from the MS analysis (Mascot Criteria) using Cytoscape software, version 2.6.3 (http://www.cytoscape.org).[20] These 45 proteins hits were first classified as untreated versus radiation (gamma+UV)-treated (Supplemental Table S3 in the Supporting Information), and the treated condition was further divided into groups according to the kinetics of the treatments, that is, 5 min, 30 min, 6 h, and 24 h (Table 2). These five groups were considered the data entry or "seed list" for the Cytoscape software using the PPPI data of *H. sapiens* available in different protein databases using the APID2NET Cytoscape Plug-in software (http://bioinfow.dep.usal.es/apid/apid2net.html).[21] The prime isolated DUSP3 network was obtained in the same way using DUS3 as the input node. (See Figure 5A.) The global PPPI network or DUSP3 Interactome (46 protein hits plus two new connections for DUSP3, either to NPM or to HnRNP C1/C2) was then analyzed with Molecular Complex Detection (MCODE) Cytoscape Plug-in software (http://baderlab.org/Software/MCODE)[22] to detect protein clusters that could be more representative of biological processes mainly related in some way to cell cycle regulation, senescence, or DNA repair.

Statistical Analyses of Network General Simplest Parameters

Each of the five temporal networks (Supplemental Figures S3–S7 in the Supporting Information) and the DUSP3 Interactome (Figure 5B) were submitted to the Network Analyzer Cytoscape plugin (http://med.bioinf.mpi-inf.mpg.de/networkanalyzer/)[23] to compare the robustness and similarity among them by observing parameters such as the clustering coefficient, connected components, radius, diameter, centralization, shortest paths, average number of neighbors, density, heterogeneity, number of nodes, isolated nodes, number of self-loops, multiedge node pairs, path length, and analysis time in seconds (Supplemental Table S3 in the Supporting Information).

Network Centralities and Gene Ontology Analyses

An analysis of network or cluster centralities was performed by checking bottleneck nodes using the Cytoscape plugin CytoHubba software (http://hub.iis.sinica.edu.tw/cytoHubba).[24] Cluster 1, which emerged from MCODE analysis, was subjected to gene ontology (GO) clustering analysis using Biological Network Gene Ontology (BiNGO) software (http://www.psb.ugent.be/cbd/papers/BiNGO/Home.html),[25] a freely available Cytoscape plugin. The degree of functional enrichment for that cluster was obtained quantitatively (p value) with the hypergeometric distribution statistical test,[26] and the multiple test correction was calculated using the false discovery rate (FDR) algorithm,[27] both of which worked independently inside of the BiNGO software application platform. Over-represented categories of biological process were obtained after FDR correction with a significance level of 0.05.

RESULTS

Investigation and Identification of New Protein Targets or Partners of DUSP3 in HeLa Cell Lysates via Pull-Down, Gel Differential Band Screening, and MS Analysis

Aside from its very classical and well-known MAPK substrates, ERK and JNK, the dual-specificity phosphatase 3 has no known nuclear targets that act in biological processes other than cell proliferation and senescence.[6] Thus, this work sought to identify DUSP3-interacting proteins directly or indirectly involved in DNA damage and repair via affinity chromatography with glutathione-sepharose beads,[28] using GST-DUSP3 as bait to pull down protein complexes containing DUSP3. We prepared lysates from unsynchronized HeLa cells with or

dx.doi.org/10.1021/pr400867j | J. Proteome Res. 2013, 12, 5851–5866

Table 1. Proteins Identified by MS from Pull-Down Experiments Using the DUSP3-WT or DUSP3-C124S Bait Proteins against Lysates from HeLa Cells with or without Exposure to Gamma or UV Irradiation[a]

Protein Identified	Score	Matches	Sequences	Coverage	Identification	Uniprot Name	Location	Function
Vimentin	1510	101	19	52%	5	VIME_HUMAN	Cytoplasm	Class-III intermediate filaments found in various cells, especially mesenchymal cells.
Dual specificity protein phosphatase 3	1463	58	8	50%	47	DUS3_HUMAN	Nucleus	Activity for phosphotyrosines. Dephosphorylates and inactivates ERK1 and ERK2.
Polyadenylate Bindin Protein 1	667	27	17	28%	2	PABP1_HUMAN	Nucleus	Implicated with other RNA-binding proteins in the cytoplasmic deadenylation/translational.
Heterogeneous Nuclear Ribonucleoprotein C1/C2	334	12	8	23%	10	HNRPC_HUMAN	Nucleus	Binds pre-mRNA. May play a role in the early steps of spliceosome assembly and pre-mRNA splicing.
Histone H2A Type 1-B/E	58	2	2	21%	1	H2A1B_HUMAN	Nucleus	Play a central role in transcription regulation, DNA repair, DNA replication and chromosomal stability.
Nucleophosmin	253	6	3	16%	3	NPM_HUMAN	Nucleus	Ribosome biogenesis, centrosome duplication, protein chaperoning, histone assembly, cell proliferation.
Histone H2B	81	2	2	15%	1	H2B1_HUMAN	Nucleus	Play a central role in transcription regulation, DNA repair, DNA replication and chromosomal stability.
Histone H1	129	3	3	15%	2	H10_HUMAN	Nucleus	Necessary for the condensation of nucleosome chains into higher-order structures.
Tubulin Alpha-1B	296	6	5	13%	2	TBA1B_HUMAN	Cytoplasm	Constituent of microtubules. Binds GTP, one at an exchangeable site on the beta chain.
Lactate Dehydrogenase	129	4	4	13%	1	LDHA_HUMAN	Cytoplasm	Catalyzes the interconversion of pyruvate and lactate with concomitant interconversion of NADH and NAD^+.
Nucleolin	328	11	9	11%	8	NUCL_HUMAN	Nucleus	It is found associated with intranucleolar chromatin and pre-ribosomal particles.
Polyadenylate Bindin Protein 3	178	11	7	11%	1	PABP3_HUMAN	Nucleus	Implicated with other RNA-binding proteins in the cytoplasmic deadenylation/translational
Histone H1.2	61	2	2	10%	2	H12_HUMAN	Nucleus	Linker DNA between nucleosomes forming the macromolecular structure known as chromatin fiber.
Atp Synthase	257	5	4	10%	1	ATPB_HUMAN	Nucleus	Mitochondrial membrane ATP synthase (F_1F_0 ATP synthase or Complex V).
Heterogeneous Nuclear Ribonucleoprotein A2/B1	203	4	3	9%	3	ROA2_HUMAN	Nucleus	Involved with pre-mRNA processing. Forms ribonucleosomes.
Enolase Alpha	212	5	3	9%	1	ENOA_HUMAN	Cytoplasm	Multifunctional enzyme playing roles in glycolysis, and in various processes such as growth control.
Histone H1.3	24	3	2	9%	1	H13_HUMAN	Nucleus	Linker DNA between nucleosomes forming the macromolecular structure known as chromatin fiber.
Tubulin Beta 5	136	4	4	9%	1	TBB5_HUMAN	Cytoplasm	Constituent of microtubules. Binds GTP, one at an exchangeable site on the beta chain.
Enolase Gama	132	4	2	7%	2	ENOG_HUMAN	Cytoplasm	Binds, in a calcium-dependent manner, promotes cell survival.
Protease Serine 4 Isoform B	66	2	2	7%	1	Q7Z5F4_HUMAN	Membrane	Probable protease. Seems to be capable of activating ENaC.
Tubulin Beta 4	136	3	3	7%	2	TBB4A_HUMAN	Cytoplasm	Constituent of microtubules.Binds GTP, one at an exchangeable site on the beta chain.
Heat Shock 70Kda Protein 8 Isoform 1	145	3	3	6%	1	HSP71_HUMAN	Cytoplasm	Stabilize proteins against aggregation; mediate the folding of newly translated polypeptides in the cytosol.
Annexin A5	76	8	2	6%	4	ANXA5_HUMAN	Nucleus	Calcium/phospholipid-binding protein which promotes membrane fusion and is involved in exocytosis.
Annexin A1	88	2	2	6%	7	ANXA1_HUMAN	Nucleus	Calcium/phospholipid-binding protein which promotes membrane fusion Is involved in exocytosis.
Polyadenylate Bindin Protein 4	118	3	3	6%	2	PABP4_HUMAN	Nucleus	Implicated with other RNA-binding proteins in the cytoplasmic deadenylation/translational
Histone H1.5	25	4	1	5%	2	H15_HUMAN	Nucleus	Linker DNA between nucleosomes forming the macromolecular structure known as the chromatin fiber.
Tyrosine-Protein Phosphatase Non-Receptor	116	3	3	5%	5	PTN11_HUMAN	Cytoplasm	Acts downstream of some receptors; participates in the signal transduction from the cell surface to nucleus.
Annexin A2	52	1	1	4%	2	ANXA2_HUMAN	Plasma	Calcium-regulated membrane-binding protein with high affinity for calcium.
The Complex Structure of the MAP Kinase	51	18	1	4%	2	MK01_HUMAN	Nucleus	MAPK1/ERK2 and MAPK3/ERK1 are the 2 MAPKs which play an important role in the MAPK/ERK cascade.
Junction Plakoglobin	55	2	2	4%	1	PLAK_HUMAN	Cytoplasm	Is important to influence the arrangement and function of the cytoskeleton.
Tubulin Beta-2A	113	2	1	4%	3	TBB2A_HUMAN	Cytoplasm	Constituent of microtubules. Binds GTP, one at an exchangeable site on the beta chain.
Elav-Like Protein 1	64	1	1	3%	2	ELAV1_HUMAN	Nucleus	Involved in 3'-UTR ARE-mediated MYC stabilization.
Heterogeneous Nuclear Ribonucleoprotein H	44	2	2	3%	1	HNRH1_HUMAN	Nucleus	Component of the hnRNP complexes providing substrates for the processing events of the pre-mRNAs.
Prohibitin PHB	71	2	1	3%	2	PHB_HUMAN	Nucleus	Prohibitin inhibits DNA synthesis. It has a role in regulating proliferation.
Tubulin Alpha 1A	99	2	1	3%	3	TBA1A_HUMAN	Cytoplasm	Constituent of microtubules. Binds GTP, one at an exchangeable site on the beta chain.
Far Upstream Element-Binding Protein 1	66	1	1	2%	1	FUBP1_HUMAN	Nucleus	Regulates MYC expression by binding to a single-stranded.
Endoplasmin	48	2	2	2%	1	ENPL_HUMAN	Cytoplasm	Chaperone that functions in the processing and transport of secreted proteins.
FubeP1	26	1	1	2%	1	Q6PJY1_HUMAN	Nucleus	RNA binding
Splicing Factor, Proline- And Glutamine- Rich	54	1	1	2%	2	SFPQ_HUMAN	Nucleus	DNA- and RNA binding protein. Essential pre-mRNA splicing factor required early in spliceosome formation.
Staphylococcal Nuclease Domain-Containing	31	2	2	2%	1	SND1_HUMAN	Nucleus	Functions as a bridging factor between STAT6 and the basal transcription factor.
CCT3 Complex Protein 1	22	1	1	2%	1	TCPG_HUMAN	Cytoplasm	Molecular chaperone; assists the folding of proteins upon ATP hydrolysis.
XRCC6 X-Ray Repair	34	2	1	2%	1	XRCC6_HUMAN	Nucleus	Involved in DNA non-homologous end joining required for double-strand break repair and V(D)J recombination.
Filamin-A	62	2	2	1%	1	FLNA_HUMAN	Cytoplasm	Anchors various transmembrane proteins to the actin cytoskeleton.
Plasminogen	45	2	1	1%	3	PLMN_HUMAN	Cytoplasm	Plasmin dissolves the fibrin of blood clots and acts as a proteolytic factor in a variety of other processes.
POTE Ankyrin Domain Family Member E	75	1	1	1%	1	POTEE_HUMAN	Nucleus	ATP binding
Vinculin	84	2	2	1%	3	VINC_HUMAN	Cytoplasm	Actin filament (F-actin)-binding protein involved in cell-matrix adhesion and cell-cell adhesion.

[a]Complementary features for the proteins include biological function and cellular localization.

without exposure to genotoxic stress by submitting the cells to gamma (5 Gy) or ultraviolet (UVA 597 J/m^2, UVB 90 J/m^2, and UVC 6 J/m^2) radiation treatments (Figure 1). These fixed low doses of radiation were selected based on biological experiments showing the presence of DNA damage and subsequent repair without leading to high levels of cell death through apoptosis or other mechanisms (Forti et al., unpublished results). Lysates from radiation-treated cells were obtained at 5 min, 30 min, 6 h, and 24 h after treatment to detect differences in the composition of protein complexes at different times following damage, recovery, and normal cell proliferation (Figure 1; Supplemental Figure S1 in the Supporting Information).

Unspecific interactions between bacterial proteins and GST were controlled using bacterial recombinant GST incubated with glutathione-sepharose beads, which were then incubated with lysates from untreated cells. Sepharose-glutahione-GST-DUSP3 beads were used as a negative control for contaminant bacterial proteins. After pulling down proteins interacting with the bait, the protein mixes were resolved on 10% SDS-PAGE gels (8 and 15% gels were also tested but were discarded due to the smaller number of protein bands found in those molecular weight ranges) followed by silver staining. Figure 1 shows a representative SDS-PAGE gel from the 30-min-after-damage condition for all tested treatments and controls using two different baits, GST-DUSP3-WT and GST-DUSP3-C124S, which contain a mutation in a catalytic cysteine residue that inactivates the phosphatase activity of DUSP3.[29] The silver-stained gels were scanned on a GE Image Scanner III, and the differential bands were analyzed by comparing the control and irradiated conditions. Bands found in any control that appeared to be the result of unspecific binding to either the sepharose beads or GST were discarded. Furthermore, multiple bands with similar molecular weights, either on the same gel or on different gels, that were pulled down independently by the wild-type or mutant bait but corresponded to the same treatment conditions were assumed to be the same protein and were pooled to obtain a more representative sample for MS analysis. Samples that were considered adequate for subsequent MS analysis were those that were systematically identified and collected from at least three independent, successful, and identical pull-down experiments. In total, 32 pull-down experiments were performed, and ~310 bands were excised and submitted to three independent MS analyses, representing all treatment conditions, including the untreated controls.

The mutated DUSP3-C124S characteristically interacts with known substrates (MAPK) and holds them ("trap mutation"),[29] thus explaining the similar banding patterns systematically observed in all gels with both the WT and C124S enzymes and, more importantly, indicating that other interactions may occur outside the catalytic site (Figure 1; Supplemental Figure S1 in the Supporting Information). The bands were excised from the gels and digested by sequence-grade modified trypsin, and the peptide analysis was performed by MS at the Mass Spectrometry facility of the National Laboratory of Biosciences (LNBio) in Campinas, SP, Brazil. The 46 identified proteins, including DUSP3 itself (shown in blue), are listed in Table 1 and classified according to the percentage of coverage, the score, the number of matched peptides relative to the original sequence in databanks, the

dx.doi.org/10.1021/pr400867j | J. Proteome Res. 2013, 12, 5851−5866

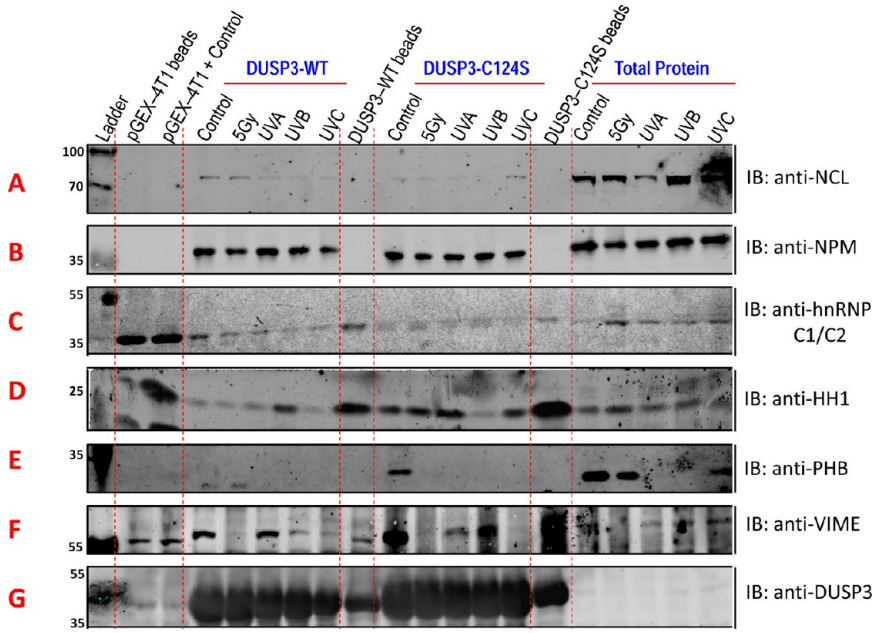

Figure 2. HeLa cell lysates obtained from different stress conditions 30 min after fixed low doses of UV and γ radiation were pulled down using DUSP3-GST and immunoblotted with specific antibodies: (A) NUCL, (B) NPM, (C) HnRNP C1/C2, (D) histone H1, (E) PHB, (F) VIME, and (G) DUSP3 as a control. Western blotting (A–F) was conducted to confirm the six protein hits obtained in the proteomic analysis, and the control was the DUSP3-GST fusion protein, which was absent from whole HeLa lysates.

entire paired peptide sequences considered for the coverage, and the number of times each protein was identified in excised bands from all three MS experiments. All hits obtained and shown in Table 1 were significant ($p < 0.05$), presenting protein scores greater than the minimum found for each hit in each individual analysis, as identified by the Mascot software analyses; all other hits that identified with very low scores were discarded.

The majority of the proteins in Table 1 exhibit nuclear localization and have biological functions related to DNA/RNA, such as structural organization, processing, synthesis, stability, and repair as well as other unrelated functions. In addition, and more importantly, these hits are not directly related to known functions or targets of DUSP3. As a proof of concept, we found ERK2 as a DUSP3 target in the MS analysis (Table 1) and also found phospho-ERK2 and phospho-JNK2 in the pull-down experiments followed by Western blots (Supplemental Figure S2 in the Supporting Information). These kinases are known to be in vitro and in vivo substrates of DUSP3 and mediate many different biological functions, such as the regulation of mitosis, proliferation, differentiation, and apoptosis. Also, the number of proteins identified as new DUSP3 targets that exhibited localization and functions related to the nucleolus was surprising, possibly indicating an unknown function of DUSP3 in this subnuclear compartment that remains unexplored but confirming our,[16] and other, previous data[6,7] showing DUSP3 to be a predominantly nuclear protein in human cervical carcinomas.

Validation of the Protein Hits by Western Blotting, Immunofluorescence, and Immunoprecipitation Reveals New Nucleolar Protein Partners Physically Interacting with DUSP3

To explore the reliability and specificity of the 46 hits identified by MS, we chose six proteins from Table 1 (shown in red) according to the following criteria: (a) four proteins [heterogeneous nuclear ribonucleoprotein C1/C2 (HnRNP C1/C2), Nucleophosmin (NPM), Nucleolin (NUCL), and Histone H1 (H1.0)] exhibiting both the highest coverage percentage and score, same nuclear localization, and related biological functions; (b) one protein, VIME, with the best MS parameters but with cytoplasmic localization and functions unrelated to DNA/RNA; and (c) one protein, prohibitin (PHB), exhibiting low coverage and scores but with localization and biological functions related to the first four chosen hits from (a). Despite these different criteria, all six proteins contain many tyrosine and threonine residues, with high probabilities of phosphorylation that have been experimentally investigated using different techniques, such as amino acid sequencing, site-directed mutagenesis, modification site-specific antibodies, and site-specific MS strategies (Supplemental Table S1 in the Supporting Information). Their presence alone indicates that DUSP3 could interact with these phosphorylation sites through its catalytic site by acting as a classic tyrosine phosphatase. Thus, we further pulled down the six proteins using GST-DUSP3-WT and GST-DUSP3-C124S and immunoblotted them with the corresponding antibodies (Figure 2). The GST-DUSP3 fusion proteins were systematically immunoblotted with anti-DUSP3 antibody as an internal control in all pull-down experiments (Figure 2G).

NUCL was among the most detected proteins in our MS analysis, and in all pull-down experiments we detected this protein interacting with DUSP3 in both untreated and in (gamma, UVA, UVB, and UVC) radiation-treated cells; however, it was never detected in the controls (Figure 2A). This surprising result is in agreement with the literature, which shows that NUCL is implicated in the genotoxic stress response and other nucleolar-dependent processes, such as tumor suppression, cell cycle control, and DNA replication and repair.[30] NPM, which is known to bind to NUCL,[31] specifically and strongly binds to DUSP3 under all conditions tested, except for under the negative control conditions (Figure 2B). HnRNP C1/C2 was also found to interact with DUSP3 under

dx.doi.org/10.1021/pr400867j | J. Proteome Res. 2013, 12, 5851–5866

treated and untreated conditions; however, the polyclonal antibody used exhibited nonspecific binding to the GST proteins in the controls (Figure 2C). HnRNP C1/C2 is also known to be involved in mRNA maturation and gene expression after DNA damage.[32] Because of this, we still did not exclude the possibility of this protein being a DUSP3 substrate/partner and sought further validation because HnRNP C1/C2 was the second most frequently detected hit in the MS analysis.

H1.0 was found to interact with DUSP3 under untreated and under all irradiated cell conditions but to interact strongly with GST controls (Figure 2D). This protein binds to DNA between the 30 nm nucleosomes,[33] and its C-terminal has also been shown to mediate many protein−protein interactions,[34] thus constituting an attractive binding partner for DUSP3. With lower specificity than Histone H1, PHB was found to weakly interact with DUSP3 in untreated cells and to a lesser extent in 5 Gy gamma-irradiated cells, whereas no binding was detected under UV conditions (Figure 2E). PHB is a tumor-suppressor protein implicated in the blockade of the G1/S cell cycle transition in human breast cancer cells, inhibiting their proliferation[35] similarly to DUSP3.[6] The last protein investigated was VIME, which is known to be phosphorylated by many kinases for the regulation of intermediate filaments and signaling pathways.[36] VIME showed binding to DUSP3 under untreated and UVA- or UVB-treated conditions but not in gamma or UVC irradiated cells (Figure 2F; Supplemental Table S2 in the Supporting Information).

Because of unspecific binding of DUSP3 to the GST protein tag observed in some controls as well as undetected DUSP3 interactions found by the immunoblots but not by MS and vice versa (Supplemental Table S2 in the Supporting Information), we decided to pursue additional experimental validation of these six proteins by confocal fluorescence microscopy (Figure 3). Because the majority of DUSP3 interactions were detected in gamma-irradiated cells, either by MS or Western blot analyses, we subsequently compared only the untreated and gamma-treated conditions. Double-labeling cells with anti-DUSP3 and anti-NUCL showed a strong colocalization of both proteins, independent of treatment, although intense staining and greater distribution in the nucleoplasm was observed in gamma-irradiated cells (Figure 3A). With regard to NPM, a specific marker for nucleoli, we found that it strongly colocalized with DUSP3 in the nucleoplasm, and in contrast with NUCL, both proteins showed a substantially higher presence in nucleoli after gamma irradiation (Figure 3B). Because NPM is known to regulate the P53 tumor suppressor, playing a positive role in the DDR triggered by ionizing and nonionizing radiation,[37] this protein seems to be a meaningful DUSP3 target in the nucleolus.

For the HnRNP C1/C2 protein, the localization appeared to not change before and after the gamma treatment and was similar to that presented by DUSP3 (Figure 3C), which is in agreement with reports showing that this protein exhibits no changes in localization after DNA damage.[32] The fact that P38 MAPK is the main kinase responsible for phosphorylating HnRNP C1/C2 in response to UV radiation[38] is also in agreement with our previous results, where DUSP3 was found to strongly colocalize with P38 MAPK after γ radiation damage (Forti et al., unpublished results). The confocal images of DUSP3 with histone H1 (Figure 3D) show a discrete nuclear colocalization of both proteins independent of the radiation treatments, similar to the results of the pull-down experiments

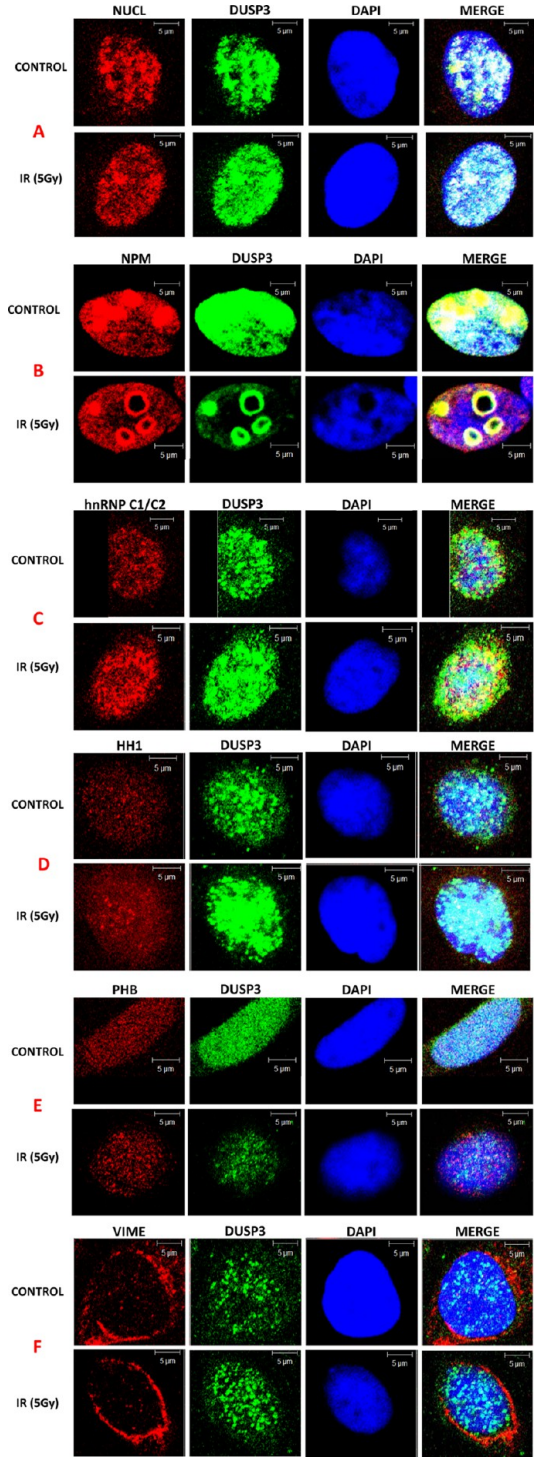

Figure 3. DUSP3 strongly colocalizes with NUCL, NPM, and HnRNP C1/C2 in the nucleolus and, more specifically, with NPM in the nucleolus after DNA damage. HeLa cells were plated on glass coverslips the day before treatment with γ radiation (5 Gy), and 30 min after irradiation they were fixed with paraformaldehyde and double-labeled by incubation with anti-DUSP3 and one of the following antibodies: (A) anti-NUCL, (B) anti-NPM, (C) anti-HnRNP C1/C2, (D) antihistone H1, (E) anti-PHB, or (F) anti-VIME. Subsequently, the cells were analyzed by fluorescence confocal microscopy using a laser scanning microscope (LSM-510 Meta, Zeiss, Germany), and photomicrographs were taken as Z-stacks from three independent experiments using the Zeiss LSM software. Representative nuclei from each condition are shown to scale.

dx.doi.org/10.1021/pr400867j | J. Proteome Res. 2013, 12, 5851−5866

(Figure 2D). Similar results were obtained for PHB, which did not significantly colocalize with DUSP3 under any condition tested. These findings are also corroborate the pull-down and Western blot assays (Figure 2E), showing that PHB appears not to interact with DUSP3 (Figure 3E), even though it has been considered an important protein for activation of the Ras-Raf-MEK-ERK pathway.[39] Afterward, VIME and DUSP3 were probed and did not show colocalization in untreated or gamma-treated cells because VIME is a primarily perinuclear and cytosolic protein and DUSP3 is almost exclusively nuclear; there is likely no direct interaction between these proteins (Figure 3F). These data partially contrast with the control and UV-treated conditions in the Western blot experiments (Figure 2F), where VIME was pulled down by DUSP3, and also with the MS results (Supplemental Table S2 in the Supporting Information), where VIME was also detected under gamma-irradiated conditions. These discrepancies are very likely the result of indirect, rapid, and transient interactions between DUSP3 and VIME.

On the basis of the results from Figures 2 and 3, we conducted a final validation to identify direct physical interactions between DUSP3 and the six hits. We immunoprecipitated DUSP3 with a monospecific anti-DUSP3 antibody to coimmunoprecipitate complexes in which DUSP3 might be participating. When probed with antibodies specific to the six proteins, a strong interaction between DUSP3 and NPM was detected, followed by a strong interaction between DUSP3 and HnRNP C1/C2, with a weaker interaction also detected between DUSP3 and NUCL (Figure 4). No significant direct interactions were detected between DUSP3 and H1.0, PHB, or VIME (not shown). These results show that DUSP3 interacts primarily with NPM and HnRNP C1/C2 or that DUSP3 can simultaneously bind very strongly to both proteins. However, because it is already known that NPM physically binds to NUCL,[40] it is likely that DUSP3 can pull down NPM and its intimate partner NUCL (in a weaker manner) as well as other proteins in that complex, even though DUSP3 does not directly interact with them. Among these proteins, we suggest H1.0, PHB, and VIME as being part of the complex in which DUSP3 might be participating because these proteins do not interact with DUSP3 and do not share the same nuclear compartments. To gain a deeper insight into why the latter proteins were systematically detected by MS and Western blot analyses after the pull-down experiments with the DUSP3 bait and how they link to the three new binding partners of DUSP3 (NPM, HnRNP C, NCL), we initiated the construction of protein–protein interaction networks using the bait and 45 prey proteins and performed an interactome analysis.

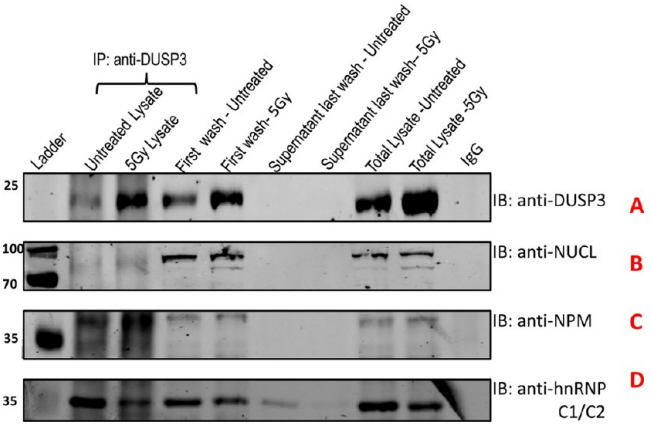

Figure 4. Co-immunoprecipitation of DUSP3 with NUCL, NPM, or HnRNP C1/C2 in untreated or 5 Gy γ radiation-treated HeLa cells. (A) DUSP3 immunoprecipitation followed by Western blot analysis with anti-DUSP3. (B) DUSP3 immunoprecipitation and Western blot analysis of NUCL (NUCL), (C) DUSP3 immunoprecipitation and Western blot analysis of NPM (NPM). (D) DUSP3I immunoprecipitation and Western blot analysis of heterogeneous nuclear ribonucleoproteins C1/C2 (HnRNP C1/C2). Western blot analysis of the total expression of DUSP3, NUCL, NPM, and HnRNP C1/C2 in untreated or 5 Gy γ radiation-treated cells after immunoprecipitation or in total cell lysates and in supernatants from the first and last washes of precipitated protein A/G beads. IgG, 5 μL of the same antibody used for immunoprecipitation, was used as a negative control in the Western blot analysis.

Physical Protein–Protein Interaction Network Substantiates DUSP3 Interactions with NPM, HnRNP C1/C2, and NUCL, Leading to an Indirect but Proximal Connection with DNA Repair and Senescence Processes

Constructing an interactome is another type of global analysis for protein–protein interactions that is very useful for confirming, reinforcing, and perhaps discarding previous results.[41−43] Therefore, we started with the construction of five networks, using the 45 protein hits plus the DUSP3 bait (shown in all networks by a black diamond) as a seed list, which were previously and initially grouped according to the different treatment types and times (Supplemental Table S2 in the Supporting Information). However, from this point on, we used the simplified comparison of untreated HeLa cell samples (control) with the treatment conditions, hereafter referred to as irradiation (gamma + UVR), as shown in Table 2, and compared them according to time post radiation.

The protein hits (Table 1) are shown in networks by colored circles (nodes), which can be repeatedly found in more than one network because they are always nested to one original condition. The connections (edges) between the nodes are represented by blue lines, which indicate physical interactions experimentally identified and confirmed by at least one appropriate biochemical technique (black number over each edge) and that are deposited in public databanks of PPPIs. In each generated network, it is possible to visualize other proteins (nodes) of different colors that have already been identified under other conditions (input proteins from another condition), in addition to the input proteins characteristic of each condition, represented by the larger circles of one specific color (Table 2). For instance, the five input proteins (represented by four purple circle nodes plus the black diamond for DUSP3) isolated by the pull-down assay and identified by MS in the 5 min condition after radiation treatments (Supplemental Figure S4 in the Supporting Information) were used to obtain the 5 min network that contains 262 nodes, with 3795 connections between them. Proteins that had already been detected and were present in the control network (Supplemental Figure S3 in the Supporting Information) were maintained in the 30 min network (Supplemental Figure S5 in the Supporting Information), but the proteins were not present in the 6 or 24 h networks (Supplemental Figures S6 and S7 in the Supporting Information). Thus, in the temporal networks built from Table 2, it is possible to observe how the DUSP3 interactome shifted over time (especially in relation to the 45 protein hits), both qualitatively and quantitatively, after the radiation

dx.doi.org/10.1021/pr400867j | J. Proteome Res. 2013, 12, 5851−5866

Table 2. Protein Groups (in red) Representing the Time Conditions Used As Inputs for the Construction of Temporal Protein−Protein Interaction Networks[a]

↓ CONDITIONS / TIME →	0 MIN	5 MIN	30 MIN	6 HS	24 HS
CONTROL	617 / 16020 18 (POTEE, Q7Z5F4) (green)				
IRRADIATIONS: GAMMA + UVA + UVB + UVC		262 / 3795 5 (purple)	862 / 18162 18 (POTEE) (brown)	686 / 15529 18 (Q7Z5F4) (red)	819 / 20400 15 (Q6PJY1) (cyano)

[a]Table also shows the number of nodes/connections (in black) found in each network (Supplemental Figures S3−S7 in the Supporting Information), and the input node colors are shown in parentheses as they appear in the network. The proteins identified by their Uniprot name/ID in red and in parentheses were not found in public PPPI databanks.

treatments (Supplemental Figures S3−S7 in the Supporting Information). Except for the 5 min condition network, which is lightly underrepresented in MS analyses (Supplemental Table S2 in the Supporting Information), all other irradiated networks showed approximately the same number of nodes, which were higher than the control condition, whereas the edge numbers were all comparable. However, the most striking changes were related to the different profiles of our MS hits found under each condition. For instance, the green nodes used as a seed list in the control condition numerically varied in the other networks as well as the red nodes from the 30 min network (Supplemental Figures S3−S7 in the Supporting Information). Statistical analyses of simple parameters from these five temporal networks show robustness and similarity among them with regard to the clustering coefficient, centralization, density, heterogeneity, and path length (Supplemental Table S3 in the Supporting Information).

Thus the actual small DUSP3 network from the PPPIs databank (Figure 5A), containing 13 nodes, 33 edges, and 12 first-degree connections in red (which is maintained in connection with and within the five temporal networks shown in Supplemental Figures S3−S7 in the Supporting Information) can now be compared with a new and updated global network that we named the "DUSP3 Interactome" (Figure 5B). The latter contains the 45 protein hits plus DUSP3 but now also includes two new interactions, as detected in our Co-IP experiments (Figure 4): DUSP3-NPM and DUSP3-HnRNP C1/C2 (DUS3-NPM and DUS3-HNRPC, respectively), detached as two red edges between two yellow nodes and the black diamond. The interaction between DUSP3 and NUCL (DUS3-NUCL) was not considered here because, as we previously described in Figure 4, despite being detected in most experiments, this interaction was weak in the Co-IP assays, suggesting that NUCL was likely bound to NPM. The DUSP3 Interactome (Figure 5B) also shows the statistical results of simple parameters (Supplemental Table S3 in the Supporting Information, right column in gray) compatible with those from Supplemental Figures S3−S7 in the Supporting Information, except for the centrality parameters that are inferior due to the network's large size (1500 nodes and 25 655 edges). Next, the DUSP3 Interactome was submitted to a cluster analysis to identify large groups of proteins densely connected in regions that may represent molecular complexes with higher affinity in biological functions. We identified 39 clusters; among the 13 higher-ranked clusters (Score >2; Supplemental Table S4 in the Supporting Information), three were unique for containing the DUSP3 protein (clusters 1, 7, and 13, shown as gray lines in Supplemental Table S4 in the Supporting Information). From these three DUSP3-containing clusters, only cluster 1, which surprisingly and coincidently presented the best score (Figure 5C; Supplemental Table S4 in the Supporting Information) and maintained the new DUSP3-NPM and DUSP3-HNRPC interactions (black diamond connecting to the two red lines), was considered for further centrality analysis by the bottleneck parameter shown in a color scale (Figure 5D). Taking into account only the top 60 best-scoring bottleneck nodes (representing 10% of the cluster 1 nodes), we constructed a new subnetwork (Figure 5E) and submitted it to a GO analysis. Thus, we were able to identify the overrepresented categories of biological processes, which were classified, grouped, and listed according to $p < 10^{-3}$ (Table 3). The results suggest this new subnetwork from cluster 1 ("new" because it now harbors DUSP3 with two novel connections experimentally identified and confirmed by this work) is generally implicated in three major biological processes that are intimately related to the structure and functions of: (i) RNA (mainly messenger and ribosomal), (ii) ribosomes (ribonucleoprotein complexes), and (iii) telomeres.

Altogether, these results suggest that DUSP3 is likely involved in DDR and repair processes[16] as well as in cellular senescence,[6] which is clear from Figure 5D based on the presence of the proteins Ku70 (also PARP1) and TERT because these proteins are intimately connected to NUCL, NPM, and HnRNP C1/C2. Furthermore, the latter new DUSP3 targets are biologically connected to other proteins that were found in our MS analyses but were not experimentally validated, including PABP1, HSP70, TBA1A, TBB5, ENOA, and PHB, which are all related to the biological processes shown in Table 3.

DISCUSSION

Because the factors that determine the in vivo substrate specificity of the are not completely known, recent efforts have been directed at identifying new substrates and elucidating the biological functions of DUSP3.[44] In this study, we performed extensive pull-downs using GST-tagged DUSP3 to detect substrates or partners of this phosphatase in cellular lysates (Figure 1; Supplemental Figure S1 in the Supporting Information). We used wild-type, full-length DUSP3, which contains the dual-specificity phosphatase catalytic domain (DSPc) plus small N- and C-terminal sequences, as well as a version mutated at cysteine 124 of the active site to detect interactions occurring along the entire length of the enzyme.[3] Total protein lysates were prepared from HeLa cells treated with or without gamma or UV radiation and screened for interacting proteins, which were identified by MS, generating a

dx.doi.org/10.1021/pr400867j | J. Proteome Res. 2013, 12, 5851−5866

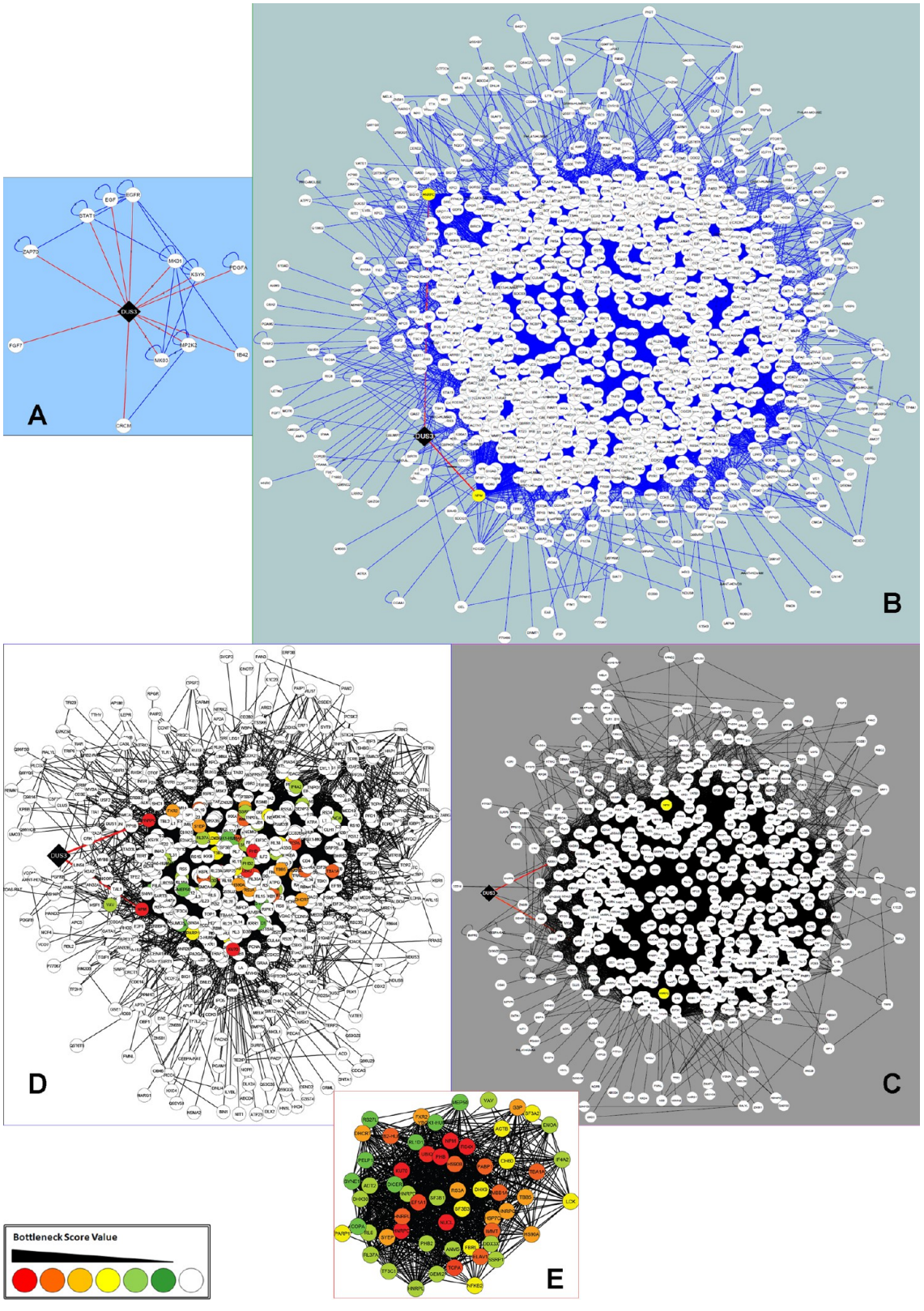

Figure 5. Updated global DUSP3 network or DUSP3 Interactome analyzed with respect to topological and statistical parameters. (A) Prime Isolated DUSP3 Network currently deposited in human PPPI databanks. The DUSP3 Interactome (B), including the 45 protein hits plus DUSP3 (black diamond) physically connected (two red edges) to NPM and HnRNP C1/C2 (two yellow circle nodes), was submitted to cluster analysis using MCODE software, and the highest scoring cluster (density × number of nodes) was identified (Supplemental Table S4 in the Supporting Information) and named Cluster 1 (C). Cluster 1 was submitted to centrality analysis using Cyto-Hubba software and classified according to the color scale shown in the rectangle (D). The top 60 highest scoring colored bottleneck nodes gave rise to a new subnetwork (E), which was submitted for gene ontology (GO) clustering analysis using BiNGO software for the identification of biological processes (Table 3).

dx.doi.org/10.1021/pr400867j | J. Proteome Res. 2013, 12, 5851−5866

Table 3. Gene Ontology (GO) Classification for All Proteins Present in Cluster 1 from the DUSP3 Interactome Summarized by 18 Biological Processes Was Obtained with the Cytoscape Plug-in BiNGO

biological process	GO identification	p value[a]	corrected p value[b]	cluster frequency[c]	total frequency[d]
RNA splicing	8380	8.33×10^{-11}	1.88×10^{-8}	39.2%	2.5%
nucleic acid metabolic process	90304	9.18×10^{-11}	1.88×10^{-8}	60.7%	10.1%
RNA stabilization	43489	1.65×10^{-10}	2.04×10^{-8}	17.8%	0.1%
regulation of RNA stability	43487	1.26×10^{-9}	1.10×10^{-7}	17.8%	0.1%
RNA processing	6396	4×10^{-9}	2.74×10^{-7}	39.2%	3.9%
cellular nitrogen compound metabolic process	34641	2.30×10^{-8}	1.29×10^{-6}	60.7%	14.5%
gene expression	10467	1.93×10^{-7}	8.53×10^{-6}	46.4%	8.8%
posttranscriptional regulation of gene expression	10608	5.93×10^{-6}	2.15×10^{-4}	28.4%	1.6%
ribonucleoprotein complex assembly	22618	1.51×10^{-5}	4.91×10^{-4}	14.2%	0.5%
ribonucleoprotein complex biogenesis	22613	5.30×10^{-4}	1.16×10^{-2}	14.2%	1.3%
telomere maintenance	723	1.55×10^{-3}	2.73×10^{-2}	7.1%	0.2%
telomere organization	32200	1.65×10^{-3}	2.83×10^{-2}	7.1%	0.2%
negative regulation of epithelial cell proliferation	50680	1.99×10^{-3}	3.23×10^{-2}	7.1%	0.2%
cellular macromolecular assembly	34622	3.14×10^{-3}	4.82×10^{-2}	14.2%	2.2%
ribosomal subunit export from nucleus	54	3.91×10^{-3}	4.82×10^{-2}	3.5%	0.0%
rRNA export from nucleus	6407	3.91×10^{-3}	4.82×10^{-2}	3.5%	0.0%
positive regulation of centrosome duplication	10825	3.91×10^{-3}	4.82×10^{-2}	3.5%	0.0%
establishment of ribosome localization	33753	3.91×10^{-3}	4.82×10^{-2}	3.5%	0.0%

[a] p value was calculated using the hypergeometric distribution of one gene ontology categories identified in the cluster. [b] Corrected p value was obtained after applying a false discovery rate algorithm. [c] Frequency with which one protein belonging to a specific gene ontology is found in the cluster. [d] Frequency with which one category of gene ontology is found in the cluster.

list of 46 protein hits, including DUSP3 itself. These proteins were classified according to their most significant proteomic data and by the frequency with which they were identified in different bands, gels, and MS analyses (Table 1). Fifty percent of the identified proteins exhibit nuclear or nuclear/cytosolic localization and are involved in DNA/RNA structure and function, whereas the others, which are more cytoplasmic, show diverse biological functions. Of these 45 hits, 6 were chosen for further experimental validation and systems biology analysis of protein−protein interactions: NPM, HnRNP C1/C2, NUCL, Histone H1, PHB, and VIME. These proteins were selected based on the criteria described above and on the presence of phosphorylatable tyrosine and threonine residues (Supplemental Table S1 in the Supporting Information) in addition to any relation to biological processes regulated by DUSP3 in human cervical cells, such as cell proliferation and senescence.[6,7]

The three best validated proteins, NUCL, NPM, and HnRNP C1/C2, are direct targets of DUSP3, as detected by MS (Table 1), Western blot (Figure 2), immunofluorescence (Figure 3), and immunoprecipitation (Figure 4) experiments. Its dual-specificity phosphatase activity allows DUSP3 to dephosphorylate a diverse array of phosphorylated proteins in many biological processes, such as cellular responses to stress, and in still unknown subcellular compartments, such as the nucleolus. Thus, one promising target for novel DUSP3 interactions is NUCL, a nucleolar phosphoprotein present in the dense fibrillar and nucleolar regions of the nucleus, representing 5% of all nucleolar protein.[45] NUCL interacted with DUSP3 under all conditions tested and, as expected, localized to the nucleus, specifically in nucleolar regions, as evidenced by confocal fluorescence microscopy showing strong colocalization with DUSP3 (Figure 3). This appears to be a direct physical interaction based on pull-down and Western blot assays (Figure 2) and is, at the very least, a secondary interaction, as evidenced by the weak bands observed in our immunoprecipitation assays (Figure 4). According to Yang et al.,[38] the stress-activated protein kinases (SAPK or JNK and P38) phosphorylate NUCL and regulate its RNA-binding ability in response to different types of genotoxic stresses, which agreed with our results showing that DUSP3 might locally dephosphorylate and downregulate these MAPKs. Similarly to other nucleolar proteins, NUCL has been implicated in cellular responses such as tumor suppression, cell cycle regulation, and DNA replication and repair, which are strongly implicated in our investigation.[46,47]

NUCL mobilizes from nucleolar regions to the nucleoplasm after exposure to IR or camptothecin treatments, stimulating the formation of protein complexes dependent on p53 that mobilize NUCL for transient replication inhibition and DNA repair.[48] In accordance with our results before and after radiation stress (Figure 3) and taking into account the fact that p53 is a key mediator of processes, such as DNA replication and repair, that also colocalizes with DUSP3 in gamma-treated HeLa cells (Forti et al., unpublished results), we infer that DUSP might participate in these processes. Additionally, it has been shown through fluorescence microscopy studies that HeLa cells overexpress the BRCA1 protein in the nucleoli and nucleoplasm and exhibit a strong colocalization of BRCA1 with NUCL.[49] This information reinforces and further highlights the interaction between DUSP3 and NUCL in repair processes, as BRCA1 has been implicated in DUSP3 downregulation and the consequent overactivation of JNK in breast cancer cells.[9] Furthermore, data from our group showed colocalization of phospho-BRCA1 (Ser1423) and DUSP3 in nucleolar regions in HeLa cells irradiated with γ radiation (Forti et al., unpublished results).

Our second hit for validation was NPM, which is considered to be the best target or partner of DUSP3 because it has been found to physically and strongly interact with DUSP3 in both untreated and gamma/UV-treated HeLa cells, according to both pull-down and immunoprecipitation experiments (Figures 2 and 4). NPM, also known as B23, is a phosphoprotein involved in various biological processes, including mRNA processing, ribosome biogenesis, cell proliferation, and

dx.doi.org/10.1021/pr400867j | J. Proteome Res. 2013, 12, 5851−5866

centrosome duplication, principally in cancer cells.[50] Experimental evidence strongly implicates NPM in cell cycle regulation through interactions with chromatin during transcriptional processes as well as via binding to histones in direct response to damage, as this protein has been found to associate with DNA damage regions.[32] The expression of NPM as well as that of the p53 and c-Jun proteins is highly induced and regulated after exposure to UV radiation, as it is associated with oncogenic activity due to its participation in processes such as growth, differentiation, DNA repair, and apoptosis.[37]

Confocal microscopy showed that NPM is dispersed in the nucleus, with preferential localization to nucleolar regions, whereas γ radiation shifted its subcompartment location, which also appears to occur for DUSP3 (Figure 3). However, neither NPM nor HnRNP C1/C2 has been shown to be actively recruited to DNA break sites, suggesting that they may respond to DNA damage through indirect mechanisms. NPM and HnRNP C1/C2 bind to chromatin after DNA damage induced by gamma/UV radiation, with NPM exclusively located in the nucleolus under normal conditions but gradually translocating and dispersing to the nucleoplasm. Furthermore, NPM did not colocalize with γ-H2AX, indicating that this protein is not actively recruited by γ-H2AX to the DNA damage foci,[32] similarly to DUSP3.[16]

Our third best characterized protein hit, HnRNP C1/C2, was systematically identified and validated by many experimental methods, independent of the treatments used in HeLa cells, and was found to interact directly with DUSP3 in pull-down and immunoprecipitation experiments (Figures 2 and 4), representing a possibly new target/partner of DUSP3. HnRNP consists of a family of RNA binding proteins that have been implicated in a variety of biological functions, including mRNA metabolism (e.g., polyadenylation and splicing) and telomere/telomerase regulation. These proteins are finely regulated during the cell cycle and are maintained at high levels for the control of RNA processing mechanisms.[51] Christian et al.[52] showed that the binding of HnRNP C1/C2 to a novel cis-acting element in the 5′-coding region of p53 mRNA regulated the expression of p53 mRNA before and during apoptosis in response to DNA damage processes in a phosphorylation-dependent manner. Lee et al.[32] have shown that HnRNP C1/C2 binds specifically and strongly to chromatin in response to DNA DSBs. The fact that HnRNP C1/C2 binds to Ku70 in an RNA-dependent manner and can be phosphorylated by DNA-PKcs and is thus involved in assisting the repair of DNA DSBs through the NHEJ pathway[32] is important for our research. These authors also reported that HnRNP C1/C2, acting as one of the main components of the nuclear matrix, does not change its location after damage, which can also be observed in our confocal microscopy data as showing colocalization with DUSP3 (Figure 3). This is also in agreement with our previous results showing the nuclear colocalization of DUSP3 with P38 MAPK after γ radiation-induced DNA damage (Forti et al., unpublished results), as this MAPK was identified as the main kinase responsible for phosphorylating HnRNP C1/C2 in response to UV-induced damage.[38]

The three other protein hits investigated in our experimental validations, H1.0, PHB, and VIME, are less related functionally and were initially chosen as controls for our experimental strategy, having been confirmed by the pull-down and MS analyses and by Western blot (Figure 2). However, the fluorescence microscopy and immunoprecipitation experiments failed to confirm colocalization or direct physical interactions with DUSP3 (Figures 3 and 4) despite the fact that these targets exhibit highly predictive tyrosine phosphorylation sites (Supplemental Table S1 in the Supporting Information). Nevertheless, these proteins unexpectedly exhibit biological functions related to the other three proteins investigated. For example, there is an α-helical domain at the N-terminal of NUCL with high analogy to other nucleolar protein domains involved in chromatin decondensation and containing variable acidic regions that interact with H1.0 through ionic interactions. These regions bind to nontranscribed DNA regions separating rRNA genes organizing nucleolar chromatin and contain phosphorylation sites for casein kinase II, cdc2, and other kinases. Consequently, the phosphorylation of NUCL appears to increase its degradation by proteases, suggesting that the stability of this protein depends on the levels of phosphorylation.[46] Similarly, H1.0 also has variable sequences as it is expressed as H1.X variants in most tissues[33] and consists of (a) a GH1 hydrophobic domain composed of three α-helices for binding to DNA and (b) less conserved N- and C- terminal regions involved in binding to nonhistone proteins with regulatory functions.[34] Thus, the role of H1.0 is still not completely understood, and only a few studies have determined a link between this protein (and the core histone octamer) and other machinery involved in determining the final structure of chromatin.[53] The weak colocalization (Figure 3) and very low immunoprecipitation of DUSP3 with H1.0 (not shown) suggest that an indirect and unknown role for this phosphatase in chromatin structure/stability should not be totally discarded.

In the case of PHB, a protein encoded by a tumor-suppressor gene highly implicated in different types of human cancers, the interaction with DUSP3 was poor in all experiments performed, including the proteomic experiments (Table 1). However, the PHB gene is located at chromosome 17q21, close to the BRCA1 locus, suggesting a role for PBH in breast cancers, where it has been shown to possess antiproliferative activity leading to cell cycle arrest at the G1/S phase transition.[35] Similarly, the DUSP3 gene is located at the same locus, and its loss is associated with similar cell cycle arrest and senescence induction.[6] PHB blocks S-phase entry in normally dividing fibroblasts or HeLa cells[54] and has also been shown to be indispensable for the activation of the Raf-MEK-ERK pathway by Ras,[39] thus indirectly correlating its biochemical functions with our validations for the DUSP3 phosphatase.

Our best hit identified by MS and the most unrelated to DUSP3 function is VIME, which is the principal constituent of type-III intermediate filaments that are known for maintaining cellular integrity and providing resistance against stress conditions. VIME is abundant in many epithelial cancers, including prostate, breast, and lung cancers as well as malignant melanoma.[36] As with other intermediate filament proteins, VIME possesses an affinity for nuclear constituents such as DNA, RNA, and histones and is structurally related to other nuclear matrix proteins and transcription factors, suggesting its involvement in DNA-based processes, such as replication, transcription, recombination, and repair.[55] VIME is phosphorylated by various kinases in vivo, and its phosphorylation state is associated with its function, including the regulation of intermediate filament structure and various signaling pathways.[36] This information suggests that VIME may act as a scaffold for nucleolar ribonucleoproteins and may thus be pulled down by the aforementioned nucleolar proteins (NUCL, NPM, and HnRNPs) or even be dephosphorylated by DUSP3

dx.doi.org/10.1021/pr400867j | J. Proteome Res. 2013, 12, 5851−5866

in a way that may regulate its function. In HeLa cells, DUSP3 is primarily nuclear, whereas VIME is mostly cytoplasmic and perinuclear (Figure 3), indicating that these proteins do not interact physically, as was also observed in our immunoprecipitation experiments (not shown).

One important finding to note from our proteomic approach was that out of 45 hits (excluding DUSP3 itself), 6 proteins (13.3%) chosen for validation were shown to be very promising and related to our biological queries regarding the involvement of DUSP3 in cell proliferation, senescence, DDR, and DNA repair processes and confirmed our MS analyses. Moreover, three (50%) of these six proteins were shown to physically interact with DUSP3, independent of the treatment used for HeLa cells. These three proteomic hits, NPM, NUCL, and HnRNP C1/C2, have already been found to bind to each other,[31,32,56−58] with strong evidence of the cooperative regulation of the cell cycle and proliferation,[31,47,59] in addition to recent evidence for their involvement in modulating DNA damage and repair processes.[60−62]

Reinforcing these observations, the systems biology analyses of PPPI networks, or interactomes,[63] of DUSP3 explored in the present work represent a very useful and powerful tool for predicting unknown interactions among proteins (known or not), specific cellular−physiological situations, molecular mechanisms, and biological/biochemical processes, especially when combined with MS data. Furthermore, indirect interactions found in the interactomes can be used to decipher whether secondary, tertiary, and even more distant protein partners of DUSP3 can lead to its unexpected participation in DNA damage and repair processes, as proposed in our research goal.[64] For example, the 45 proteins identified in our MS analysis were grouped according to treatment (UV + γ radiation) duration (Table 2 and Supplemental Table S2 in the Supporting Information) and used to generate the temporal networks shown in Supplemental Figures S3−S7 in the Supporting Information, which clearly show that the prime isolated DUSP3 network (Figure 5A) connects to many other proteins in a very conservative way. However, the 45 hits (colored circles) oscillate around DUSP3 over time and also appear under the untreated conditions (Supplemental Figures S3−S7 in the Supporting Information). In fact, statistical analyses of these results (Supplemental Table S3 in the Supporting Information) indicate that the robustness of our DUSP3 networks can be used to confirm the MS data. Taking advantage of our best validated results, namely, the DUSP3-NPM and DUSP3-HnRNPC interactions, we constructed the DUSP3 Interactome (Figure 5B), wherein we identified a small cluster (Supplemental Table S4 in the Supporting Information and Figure 5C) containing DUSP3 and many protein hits (not completely validated) acting as large hubs (highest scored bottlenecks) controlling three major biological processes closely related to the structure and function of RNAs, ribosomes, and telomeres (Figures 5D,E; Table 3).

Considering all of the experimental and systems biology data obtained in this work, we are confident in suggesting that DUSP3, rather than being distant and unrelated, plays an intimate role in DDR/repair processes[16] in addition to mediating cellular senescence.[6] We are confident in these roles for DUSP3 because, in the subnetwork formed by the highest scored bottleneck nodes (Figure 5E), it is possible to observe the Ku70 and TERT proteins directly interacting with NUCL, NPM, and HnRNP C1/C2, and, as previously reported, NUCL interacts with the human telomerase reverse transcriptase subunit (hTERT) and alters its subcellular localization. This interaction is critical for the nucleolar localization of hTERT and the dynamic intracellular localization of the telomerase complex,[40] which was shown to be negatively affected by the loss of DUSP3 in HeLa cells.[6] Similarly, telomerase activity and the regulation of telomere length by the telomerase complex are dependent on functional HnRNP C1/C2 proteins[65] as well as on Ku70/80, which associates with hTERT and might function to regulate the access of telomerase to telomeric DNA ends.[66] On this point, our results suggest the possible involvement of DUSP3 in telomere DNA repair and senescence mechanisms.[67,68] Finally, and also in agreement with data reported by others,[61] these novel DUSP3 targets (NPM, NUCL, and HnRNP C1/C2) are biologically connected to (a) other proteins found in our MS analyses, such as PABP1, HSP70, TBA1A, TBB5, ENOA, and PHB; (b) to proteins specifically involved in nucleolar functions (HnRNP D, L, Q, U); and (c) to other proteins involved in cell proliferation and DNA repair, such as PARP1 and PHB2 as well as BARD1 and B-Raf1 (Table 2; Figure 5D,E).

On balance, the results of this search for novel protein targets or partners of dual-specificity phosphatase 3 open new possibilities regarding other tyrosine phosphates regulating important nuclear or nucleolar functions in human cells. These results can be clarified by future investigations at biological, molecular, and mechanistic levels. For instance, DUSP3 is the human homologue of VH1, a dual-specificity phosphatase encoded by the *Vaccinia virus*, the repression of which strongly reduces the infectivity of these viral particles. This reduced infectivity is thought to occur via the regulation of viral gene transcription either in vitro or in vivo by VH1 through the dephosphorylation of an 11 kDa hyperphosphorylated protein product of the F18 viral gene.[69] Concurrently, many reports show that viruses target the nucleolus and its components to facilitate infection. Viruses interact with the nucleoli of the host cells, and viral proteins (such as VH1 in the case of *Vaccinia*) can colocalize with nucleolar proteins, such as fibrillarin, NPM, and NUCL, promoting their redistribution and incorporating these proteins into the viral replication machinery. Because the nucleolus is implicated in the regulation of processes such as the cell cycle, many viruses target this subnuclear compartment to alter the host cell cycle and make it more favorable for viral replication and infectivity. Thus, according to our results, DUSP3 might play a role in the nucleolus similar to that of its homologue, VH1.

■ ASSOCIATED CONTENT

Supporting Information

HeLa cell lysates with the indicated gamma and UV treatments were pulled down using DUSP-GST bait and resolved on SDS-PAGE gels followed by silver staining for protein band isolation and identification. Identification of the known DUSP3 substrates ERK2 and JNK2 in the phosphorylated state using the pull-down technique. The DUSP3 Interactome of HeLa cells under the control condition and 5 min, 30 min, 6 h, and 24 h after gamma and UV irradiation of HeLa cells. Phosphotyrosine and phosphothreonine residues in the sequences of the six protein hits identified using experimental phosphopeptides databases and confirmed by prediction software in three different species for homology visualization. The 45 protein hits identified in all three mass spectrometry

dx.doi.org/10.1021/pr400867j | J. Proteome Res. 2013, 12, 5851−5866

analyses from the different cell lysate conditions. Analysis of the DUSP3 networks showing that simpler network parameters are well maintained over time after radiation damage. Clustering analysis of the global network revealed 13 higher scoring clusters, three of which contained DUSP3. This material is available free of charge via the Internet at http://pubs.acs.org.

AUTHOR INFORMATION

Corresponding Author

*Phone: 55-11-3091-9905. Fax: 55-11-3091-2186. E-mail: flforti@iq.usp.br.

Present Address

§F.L.F.: Av. Prof. Lineu Prestes, 748 - Bl.09i, Sl.922 CEP: 05508−900 - Cidade Universitária - São Paulo-SP, Brazil.

Funding

Funds from Fundação Universidade Federal do ABC (UFABC), Fundação de Amparo à Pesquisa do Estado de São Paulo (FAPESP), and the University of São Paulo through the Núcleo de Apoio à Pesquisa na Interface Proteólise Sinalização Celular (NAPPS) supported the research presented in this manuscript.

Notes

The authors declare no competing financial interest.

ACKNOWLEDGMENTS

K.P. was a recipient of the Fundação UFABC Master's degree fellowship. This research was supported by the Brazilian agency FAPESP, grant #2008/58264-5 to F.L.F. as a Young Investigator. We thank Andressa P. Costa and Viviane Machtura for technical assistance. We thank Dr. Margarida M. Hamada, Elizabeth Somessari, and all of the staff from the Radiation Technology Center of the IPEN/CNEN, Sao Paulo-SP, Brazil for performing the gamma irradiations. We thank Dr. Adriana Franco Paes Leme and all of the staff from the Mass Spectrometry Facility of the Brazilian Biosciences National Laboratory (LNBio), Campinas-SP, Brazil, for the MS analyses. We also thank the AJE staff and editors for providing editing services.

ABBREVIATIONS

DDR, DNA damage response; DME, Dulbecco's modified Eagle; DSB, double-strand break; FDR, false discovery rate; GO, gene ontology; HR, homologous recombination; IPTG, isopropyl β-D-1-thiogalactopyranoside; IR, ionizing radiation; MS, mass spectrometry; NHEJ, nonhomologous end joining; PPPI, physical protein−protein interaction; SSB, single-strand break; WT, wild type

REFERENCES

(1) Hunter, T. Protein kinases and phosphatases: the yin and yang of protein phosphorylation and signaling. *Cell* **1995**, *80* (2), 225−36.
(2) Zhang, Z. Y. Protein tyrosine phosphatases: prospects for therapeutics. *Curr. Opin. Chem. Biol.* **2001**, *5* (4), 416−23.
(3) Patterson, K. I.; Brummer, T.; O'Brien, P. M.; Daly, R. J. Dual-specificity phosphatases: critical regulators with diverse cellular targets. *Biochem. J.* **2009**, *418* (3), 475−89.
(4) Worby, C. A.; Gentry, M. S.; Dixon, J. E. Laforin, a dual specificity phosphatase that dephosphorylates complex carbohydrates. *J. Biol. Chem.* **2006**, *281* (41), 30412−8.
(5) Maehama, T.; Dixon, J. E. The tumor suppressor, PTEN/MMAC1, dephosphorylates the lipid second messenger, phosphatidylinositol 3,4,5-trisphosphate. *J. Biol. Chem.* **1998**, *273* (22), 13375−8.
(6) Rahmouni, S.; Cerignoli, F.; Alonso, A.; Tsutji, T.; Henkens, R.; Zhu, C.; Louis-dit-Sully, C.; Moutschen, M.; Jiang, W.; Mustelin, T. Loss of the VHR dual-specific phosphatase causes cell-cycle arrest and senescence. *Nat. Cell Biol.* **2006**, *8* (5), 524−31.
(7) Henkens, R.; Delvenne, P.; Arafa, M.; Moutschen, M.; Zeddou, M.; Tautz, L.; Boniver, J.; Mustelin, T.; Rahmouni, S. Cervix carcinoma is associated with an up-regulation and nuclear localization of the dual-specificity protein phosphatase VHR. *BMC Cancer* **2008**, *8*, 147.
(8) Arnoldussen, Y. J.; Lorenzo, P. I.; Pretorius, M. E.; Waehre, H.; Risberg, B.; Maelandsmo, G. M.; Danielsen, H. E.; Saatcioglu, F. The mitogen-activated protein kinase phosphatase vaccinia H1-related protein inhibits apoptosis in prostate cancer cells and is overexpressed in prostate cancer. *Cancer Res.* **2008**, *68* (22), 9255−64.
(9) Hao, L.; ElShamy, W. M. BRCA1-IRIS activates cyclin D1 expression in breast cancer cells by downregulating the JNK phosphatase DUSP3/VHR. *Int. J. Cancer* **2007**, *121* (1), 39−46.
(10) Yuvaniyama, J.; Denu, J. M.; Dixon, J. E.; Saper, M. A. Crystal structure of the dual specificity protein phosphatase VHR. *Science* **1996**, *272* (5266), 1328−31.
(11) Alonso, A.; Saxena, M.; Williams, S.; Mustelin, T. Inhibitory role for dual specificity phosphatase VHR in T cell antigen receptor and CD28-induced Erk and Jnk activation. *J. Biol. Chem.* **2001**, *276* (7), 4766−71.
(12) Gerlitz, G. HMGNs, DNA repair and cancer. *Biochim. Biophys. Acta* **2010**, *1799* (1−2), 80−5.
(13) Kim, M. J.; Choi, S. Y.; Park, I. C.; Hwang, S. G.; Kim, C.; Choi, Y. H.; Kim, H.; Lee, K. H.; Lee, S. J. Opposing roles of c-Jun NH2-terminal kinase and p38 mitogen-activated protein kinase in the cellular response to ionizing radiation in human cervical cancer cells. *Mol Cancer Res* **2008**, *6* (11), 1718−31.
(14) Golding, S. E.; Rosenberg, E.; Neill, S.; Dent, P.; Povirk, L. F.; Valerie, K. Extracellular signal-related kinase positively regulates ataxia telangiectasia mutated, homologous recombination repair, and the DNA damage response. *Cancer Res.* **2007**, *67* (3), 1046−53.
(15) Lu, C.; Zhu, F.; Cho, Y. Y.; Tang, F.; Zykova, T.; Ma, W. Y.; Bode, A. M.; Dong, Z. Cell apoptosis: requirement of H2AX in DNA ladder formation, but not for the activation of caspase-3. *Mol. Cell* **2006**, *23* (1), 121−32.
(16) F., F. L.; N., M. H. M.; T., T. E. P. Investigating roles of dual tyrosine phosphatases in DNA damage responses. *Int. J. Low Radiat.* **2010**, *4*, 8.
(17) Forti, F. L.; Armelin, H. A. Vasopressin triggers senescence in K-ras transformed cells via RhoA-dependent downregulation of cyclin D1. *Endocr.-Relat. Cancer* **2007**, *14* (4), 1117−25.
(18) Mortz, E.; Krogh, T. N.; Vorum, H.; Gorg, A. Improved silver staining protocols for high sensitivity protein identification using matrix-assisted laser desorption/ionization-time of flight analysis. *Proteomics* **2001**, *1* (11), 1359−63.
(19) Aragao, A. Z.; Nogueira, M. L.; Granato, D. C.; Simabuco, F. M.; Honorato, R. V.; Hoffman, Z.; Yokoo, S.; Laurindo, F. R.; Squina, F. M.; Zeri, A. C.; Oliveira, P. S.; Sherman, N. E.; Paes Leme, A. F. Identification of novel interaction between ADAM17 (a disintegrin and metalloprotease 17) and thioredoxin-1. *J. Biol. Chem.* **2012**, *287* (51), 43071−82.
(20) Shannon, P.; Markiel, A.; Ozier, O.; Baliga, N. S.; Wang, J. T.; Ramage, D.; Amin, N.; Schwikowski, B.; Ideker, T. Cytoscape: a software environment for integrated models of biomolecular interaction networks. *Genome Res.* **2003**, *13* (11), 2498−504.
(21) Hernandez-Toro, J.; Prieto, C.; De las Rivas, J. APID2NET: unified interactome graphic analyzer. *Bioinformatics* **2007**, *23* (18), 2495−7.
(22) Bader, G. D.; Hogue, C. W. An automated method for finding molecular complexes in large protein interaction networks. *BMC Bioinformatics* **2003**, *4*, 2.
(23) Assenov, Y.; Ramirez, F.; Schelhorn, S. E.; Lengauer, T.; Albrecht, M. Computing topological parameters of biological networks. *Bioinformatics* **2008**, *24* (2), 282−4.

(24) Lin, C. Y.; Chin, C. H.; Wu, H. H.; Chen, S. H.; Ho, C. W.; Ko, M. T. Hubba: hub objects analyzer–a framework of interactome hubs identification for network biology. *Nucleic Acids Res.* **2008**, *36* (Web Server issue), W438–43.
(25) Maere, S.; Heymans, K.; Kuiper, M. BiNGO: a Cytoscape plugin to assess overrepresentation of gene ontology categories in biological networks. *Bioinformatics* **2005**, *21* (16), 3448–9.
(26) Rice, J. A. *Mathematical Statistics and Data Analysis*, 3rd ed.; Duxbury Press: Belmont, CA, 2007.
(27) Benjamini, Y.; Yekutieli, D. The control of the false discovery rate in multiple testing under dependency. *Ann. Stat.* **2001**, *4*, 23.
(28) Einarson, M. B.; Pugacheva, E. N.; Orlinick, J. R. Identification of Protein-Protein Interactions with Glutathione-S-Transferase (GST) Fusion Proteins. *Cold Spring Harbor Protoc. 2007* **2007**, DOI: 10.1101/pdb.top11.
(29) Todd, J. L.; Rigas, J. D.; Rafty, L. A.; Denu, J. M. Dual-specificity protein tyrosine phosphatase VHR down-regulates c-Jun N-terminal kinase (JNK). *Oncogene* **2002**, *21* (16), 2573–83.
(30) Gueven, N.; Becherel, O. J.; Kijas, A. W.; Chen, P.; Howe, O.; Rudolph, J. H.; Gatti, R.; Date, H.; Onodera, O.; Taucher-Scholz, G.; Lavin, M. F. Aprataxin, a novel protein that protects against genotoxic stress. *Hum. Mol. Genet.* **2004**, *13* (10), 1081–93.
(31) Liu, H. T.; Yung, B. Y. In vivo interaction of nucleophosmin/B23 and protein C23 during cell cycle progression in HeLa cells. *Cancer Lett* **1999**, *144* (1), 45–54.
(32) Lee, S. Y.; Park, J. H.; Kim, S.; Park, E. J.; Yun, Y.; Kwon, J. A proteomics approach for the identification of nucleophosmin and heterogeneous nuclear ribonucleoprotein C1/C2 as chromatin-binding proteins in response to DNA double-strand breaks. *Biochem. J.* **2005**, *388* (Pt1), 7–15.
(33) Marino-Ramirez, L.; Levine, K. M.; Morales, M.; Zhang, S.; Moreland, R. T.; Baxevanis, A. D.; Landsman, D. The Histone Database: an integrated resource for histones and histone fold-containing proteins. *Database* **2011**, *2011*, bar048.
(34) Wisniewski, J. R.; Zougman, A.; Kruger, S.; Mann, M. Mass spectrometric mapping of linker histone H1 variants reveals multiple acetylations, methylations, and phosphorylation as well as differences between cell culture and tissue. *Mol. Cell. Proteomics* **2007**, *6* (1), 72–87.
(35) Wang, S.; Zhang, B.; Faller, D. V. Prohibitin requires Brg-1 and Brm for the repression of E2F and cell growth. *EMBO J.* **2002**, *21* (12), 3019–28.
(36) Satelli, A.; Li, S. Vimentin in cancer and its potential as a molecular target for cancer therapy. *Cell. Mol. Life Sci.* **2011**, *68* (18), 3033–46.
(37) Wu, M. H.; Yung, B. Y. UV stimulation of nucleophosmin/B23 expression is an immediate-early gene response induced by damaged DNA. *J. Biol. Chem.* **2002**, *277* (50), 48234–40.
(38) Yang, C.; Maiguel, D. A.; Carrier, F. Identification of nucleolin and nucleophosmin as genotoxic stress-responsive RNA-binding proteins. *Nucleic Acids Res.* **2002**, *30* (10), 2251–60.
(39) Rajalingam, K.; Wunder, C.; Brinkmann, V.; Churin, Y.; Hekman, M.; Sievers, C.; Rapp, U. R.; Rudel, T. Prohibitin is required for Ras-induced Raf-MEK-ERK activation and epithelial cell migration. *Nat. Cell Biol.* **2005**, *7* (8), 837–43.
(40) Khurts, S.; Masutomi, K.; Delgermaa, L.; Arai, K.; Oishi, N.; Mizuno, H.; Hayashi, N.; Hahn, W. C.; Murakami, S. Nucleolin interacts with telomerase. *J. Biol. Chem.* **2004**, *279* (49), 51508–15.
(41) Archakov, A. I.; Govorun, V. M.; Dubanov, A. V.; Ivanov, Y. D.; Veselovsky, A. V.; Lewi, P.; Janssen, P. Protein-protein interactions as a target for drugs in proteomics. *Proteomics* **2003**, *3* (4), 380–91.
(42) Wodak, S. J.; Pu, S.; Vlasblom, J.; Seraphin, B. Challenges and rewards of interaction proteomics. *Mol. Cell. Proteomics* **2009**, *8* (1), 3–18.
(43) Raman, K. Construction and analysis of protein-protein interaction networks. *Autom. Exp.* **2010**, *2* (1), 2.
(44) Luechapanichkul, R.; Chen, X.; Taha, H. A.; Vyas, S.; Guan, X.; Freitas, M. A.; Hadad, C. M.; Pei, D. Specificity profiling of dual specificity phosphatase vaccinia VH1-related (VHR) reveals two distinct substrate binding modes. *J. Biol. Chem.* **2013**, *288* (9), 6498–510.
(45) Lapeyre, B.; Bourbon, H.; Amalric, F. Nucleolin, the major nucleolar protein of growing eukaryotic cells: an unusual protein structure revealed by the nucleotide sequence. *Proc. Natl. Acad. Sci. U. S. A.* **1987**, *84* (6), 1472–6.
(46) Srivastava, M.; Pollard, H. B. Molecular dissection of nucleolin's role in growth and cell proliferation: new insights. *FASEB J* **1999**, *13* (14), 1911–22.
(47) Pinol-Roma, S. Association of nonribosomal nucleolar proteins in ribonucleoprotein complexes during interphase and mitosis. *Mol. Biol. Cell* **1999**, *10* (1), 77–90.
(48) Daniely, Y.; Dimitrova, D. D.; Borowiec, J. A. Stress-dependent nucleolin mobilization mediated by p53-nucleolin complex formation. *Mol. Cell. Biol.* **2002**, *22* (16), 6014–22.
(49) Tulchin, N.; Chambon, M.; Juan, G.; Dikman, S.; Strauchen, J.; Ornstein, L.; Billack, B.; Woods, N. T.; Monteiro, A. N. BRCA1 protein and nucleolin colocalize in breast carcinoma tissue and cancer cell lines. *Am. J. Pathol.* **2010**, *176* (3), 1203–14.
(50) Grisendi, S.; Mecucci, C.; Falini, B.; Pandolfi, P. P. Nucleophosmin and cancer. *Nat. Rev. Cancer* **2006**, *6* (7), 493–505.
(51) Fay, J.; Kelehan, P.; Lambkin, H.; Schwartz, S. Increased expression of cellular RNA-binding proteins in HPV-induced neoplasia and cervical cancer. *J. Med. Virol.* **2009**, *81* (5), 897–907.
(52) Christian, K. J.; Lang, M. A.; Raffalli-Mathieu, F. Interaction of heterogeneous nuclear ribonucleoprotein C1/C2 with a novel cis-regulatory element within p53 mRNA as a response to cytostatic drug treatment. *Mol. Pharmacol.* **2008**, *73* (5), 1558–67.
(53) Vaquero, A.; Scher, M.; Lee, D.; Erdjument-Bromage, H.; Tempst, P.; Reinberg, D. Human SirT1 interacts with histone H1 and promotes formation of facultative heterochromatin. *Mol. Cell* **2004**, *16* (1), 93–105.
(54) Roskams, A. J.; Friedman, V.; Wood, C. M.; Walker, L.; Owens, G. A.; Stewart, D. A.; Altus, M. S.; Danner, D. B.; Liu, X. T.; McClung, J. K. Cell cycle activity and expression of prohibitin mRNA. *J. Cell. Physiol.* **1993**, *157* (2), 289–95.
(55) Hartig, R.; Shoeman, R. L.; Janetzko, A.; Tolstonog, G.; Traub, P. DNA-mediated transport of the intermediate filament protein vimentin into the nucleus of cultured cells. *J. Cell Sci.* **1998**, *111* (Pt 24), 3573–84.
(56) Derenzini, M.; Sirri, V.; Pession, A.; Trere, D.; Roussel, P.; Ochs, R. L.; Hernandez-Verdun, D. Quantitative changes of the two major AgNOR proteins, nucleolin and protein B23, related to stimulation of rDNA transcription. *Exp. Cell Res.* **1995**, *219* (1), 276–82.
(57) Li, Y. P.; Busch, R. K.; Valdez, B. C.; Busch, H. C23 interacts with B23, a putative nucleolar-localization-signal-binding protein. *Eur. J. Biochem.* **1996**, *237* (1), 153–8.
(58) Brockstedt, E.; Rickers, A.; Kostka, S.; Laubersheimer, A.; Dorken, B.; Wittmann-Liebold, B.; Bommert, K.; Otto, A. Identification of apoptosis-associated proteins in a human Burkitt lymphoma cell line. Cleavage of heterogeneous nuclear ribonucleoprotein A1 by caspase 3. *J. Biol. Chem.* **1998**, *273* (43), 28057–64.
(59) Peter, M.; Nakagawa, J.; Doree, M.; Labbe, J. C.; Nigg, E. A. Identification of major nucleolar proteins as candidate mitotic substrates of cdc2 kinase. *Cell* **1990**, *60* (5), 791–801.
(60) Du, Y. C.; Gu, S.; Zhou, J.; Wang, T.; Cai, H.; Macinnes, M. A.; Bradbury, E. M.; Chen, X. The dynamic alterations of H2AX complex during DNA repair detected by a proteomic approach reveal the critical roles of Ca(2+)/calmodulin in the ionizing radiation-induced cell cycle arrest. *Mol. Cell. Proteomics* **2006**, *5* (6), 1033–44.
(61) Nalabothula, N.; Indig, F. E.; Carrier, F. The Nucleolus Takes Control of Protein Trafficking Under Cellular Stress. *Mol. Cell. Pharmacol* **2010**, *2* (5), 203–212.
(62) Nalabothula, N.; Chakravarty, D.; Pierce, A.; Carrier, F. Over Expression of Nucleophosmin and Nucleolin Contributes to the Suboptimal Activation of a G2/M Checkpoint in Ataxia Telangiectasia Fibroblasts. *Mol. Cell. Pharmacol* **2010**, *2* (5), 179–189.

(63) Vidal, M.; Cusick, M. E.; Barabasi, A. L. Interactome networks and human disease. *Cell* **2011**, *144* (6), 986−98.
(64) Pescatore, L. A.; Bonatto, D.; Forti, F. L.; Sadok, A.; Kovacic, H.; Laurindo, F. R. Protein disulfide isomerase is required for platelet-derived growth factor-induced vascular smooth muscle cell migration, Nox1 NADPH oxidase expression, and RhoGTPase activation. *J. Biol. Chem.* **2012**, *287* (35), 29290−300.
(65) Fu, D.; Collins, K. Purification of human telomerase complexes identifies factors involved in telomerase biogenesis and telomere length regulation. *Mol. Cell* **2007**, *28* (5), 773−85.
(66) Chai, W.; Ford, L. P.; Lenertz, L.; Wright, W. E.; Shay, J. W. Human Ku70/80 associates physically with telomerase through interaction with hTERT. *J. Biol. Chem.* **2002**, *277* (49), 47242−7.
(67) Lansdorp, P. M. Repair of telomeric DNA prior to replicative senescence. *Mech. Ageing Dev.* **2000**, *118* (1−2), 23−34.
(68) Nandakumar, J.; Cech, T. R. Finding the end: recruitment of telomerase to telomeres. *Nat. Rev. Mol. Cell Biol.* **2013**, *14* (2), 69−82.
(69) Liu, K.; Lemon, B.; Traktman, P. The dual-specificity phosphatase encoded by vaccinia virus, VH1, is essential for viral transcription in vivo and in vitro. *J. Virol.* **1995**, *69* (12), 7823−34.